Definition of the Moist-Air Exergy Norm: A Comparison with Existing "Moist Energy Norms"

Pascal Marquet, Jean-François Mahfouf, Daniel Holdaway

▶ To cite this version:

HAL Id: **meteo-03353517**

https://meteofrance.hal.science/meteo-03353517

Submitted on 24 Sep 2021

Definition of the moist-air exergy norm:
a comparison with existing "moist energy norms".

by Pascal Marquet [(1)], Jean-François Mahfouf [(1)], Daniel Holdaway [(2)].

[(1)] Météo-France CNRM/GMAP / CNRS UMR3589. Toulouse. France.
[(2)] Global Modeling and Assimilation Office, NASA Goddard Space Flight Center, Greenbelt, Maryland and University Corporation for Atmospheric Research, Boulder, Colorado.

E-mail: pascal.marquet@meteo.fr

Abstract

This study presents a new formulation for the norms and scalar products used in tangent linear or adjoint models to determine forecast errors and sensitivity to observations and to calculate singular vectors. The new norm is derived from the concept of moist-air available enthalpy, which is one of the availability functions referred to as exergy in general thermodynamics. It is shown that the sum of the kinetic energy and the moist-air available enthalpy can be used to define a new moist-air squared norm which is quadratic in: 1) wind components; 2) temperature; 3) surface pressure; and 4) water vapor content. Preliminary numerical applications are performed to show that the new weighting factors for temperature and water vapor are significantly different from those used in observation impact studies, and are in better agreement with observed analysis increments. These numerical applications confirm that the weighting factors for water vapor and temperature exhibit a large increase with height (by several orders of magnitude) and a minimum in the middle troposphere, respectively.

1   Introduction.

Several inner-products, based on "energy" squared norms, have been used in four-dimensional variational assimilation tools to minimize cost functions (Talagrand, 1981; Courtier, 1987; Thépaut and Courtier, 1991). It was supposed that the "energy" corresponding to observational errors could be distributed equally among these different basic prognostic fields. Inner-products based on these "energy" squared norms are used to define dry semi-implicit operators and dry normal modes of GCMs or NWP models, as long as they are invariant by the linear set of primitive equations (Thépaut and Courtier, 1991).

Here, the term "energy" means that the sum of quadratic terms is considered for perturbations of the wind components $(u')^2 + (v')^2$, temperature $(T')^2$ and surface pressure $(p'_s)^2$ or $[\ln(p_s)']^2$ (see appendix A for the list of symbols). Moist-air generalizations of the "energy" squared norm have been suggested by Courtier (1987, hereafter C87), Ehrendorfer et al. (1999, hereafter E99) or Mahfouf and Bilodeau (2007, hereafter MB07), among others, by including the water vapor content via an additional quadratic term $(q'_v)^2$.

The same inner-products and norms are currently used for computing dry or moist singular vectors and for determining forecast errors or sensitivity to observations based on tangent linear and adjoint models (Buizza and Palmer, 1995; Palmer et al., 1998; Mahfouf and Bilodeau, 2007; Janisková and Cardinali, 2017).

However, all these norms suffer from a lack of consistency with physical relationships in thermodynamics, because: i) these "energy" squared norms are not based on the standard definition of energy as expressed in general thermodynamics; ii) the use of the squared norm for water including the quadratic term $(q'_v)^2$ is poorly justified; iii) these definitions are not unique, with for instance an arbitrary tuning parameters which is often left undetermined for the water component.

Ideally, all these quadratic terms should be derived from some general laws of physics. This is true for the

average of the kinetic energy $(\overline{u^2} + \overline{v^2})/2$, which is the sum of the terms $(\overline{u})^2/2 + (\overline{v})^2/2$ computed with the mean state of wind plus the terms $\overline{(u')^2}/2 + \overline{(v')^2}/2$ computed with the perturbations of wind. This result is true if $u' = u - \overline{u}$ and $v' = v - \overline{v}$, leading to $\overline{(u')} = \overline{(v')} = 0$. The squared norm for the wind components is computed in assimilation, singular vector and sensitivity studies with $\overline{(u')^2}/2 + \overline{(v')^2}/2$, where for instance u' and v' are the unbiased departures between analyses and short-range forecasts.

In contrast, the usual temperature component of the squared norm $\overline{(T^2)}/2 = (\overline{T})^2/2 + \overline{(T')^2}/2$ cannot be derived from the general definition of the energy and the first law of thermodynamics. Indeed, the dry-air internal energy or enthalpy varies linearly with temperature, with $h \approx c_{pd}\,T$ for the enthalpy up to constant reference values. Consequently, the true energy and enthalpy cannot generate quadratic terms, due to $\overline{h'} = c_{pd}\,\overline{T'} = 0$.

In order to derive quadratic squared norms in both wind components and temperature, a relevant method might be based on the study of the sum of the kinetic energy and "a form of the Available Potential Energy" (APE) of Lorenz (1955). This method is chosen in Talagrand (1981), the old ARPEGE-IFS documentation (1989, unpublished), Joly and Thorpe (1991), Joly (1995), Ehrendorfer and Errico (1995), Errico and Ehrendorfer (1995), E99, Ehrendorfer (2000), Errico (2000) and Descamps et al. (2007).

In these studies, the specific value of the approximate APE is written as $\overline{(T')^2}/(2\,\overline{\Gamma})$, where both the perturbation of temperature $T' = T - \overline{T}$ and the stability parameter $\overline{\Gamma}$ depend on $\overline{T}$, where

$$\overline{\Gamma} \;=\; \frac{\overline{T}}{c_{pd}} \;-\; \frac{p}{R_d}\,\frac{\partial\,\overline{T}}{\partial\,p} \;. \tag{1}$$

The calculations of $\overline{\Gamma}$ are explicitly performed in Talagrand (1981) and Descamps et al. (2007) by using a standard atmosphere for defining a reference profile $\overline{T}(p)$ which varies with height.

On the other hand, the stability parameter is often computed by using a constant reference value for $\overline{T}$, which is denoted by T_r or an equivalent. This leads to $\partial\,\overline{T}/\partial\,p = 0$ in (1) and to $\overline{\Gamma} = T_r/c_{pd}$. This is an explanation for the quadratic term

$$\frac{\overline{(T')^2}}{2\,\overline{\Gamma}} \;=\; c_{pd}\,\frac{\overline{(T')^2}}{2\,T_r} \tag{2}$$

which is retained in almost all present formulations of the temperature component of norms. A con-

stant value T_r is used in Courtier (1987), Thépaut and Courtier (1991), Buizza et al. (1993), Ehrendorfer and Errico (1995), Buizza et al. (1996), Mahfouf and Buizza (1996), E99, Errico (2000), Barkmeijer et al. (2001), Zadra et al. (2004), Errico et al. (2004), Mahfouf and Bilodeau (2007), Rivière et al. (2009), Holdaway et al. (2014), Janisková and Cardinali (2017), among others.

However, it is worth noting that the use of a constant value T_r for $\overline{T}(p)$ in (2) is not compatible with the stability term (1) that appears in the formulation of APE expressed with pressure coordinate, where $\overline{T}$ must be defined as the isobaric average of T according to Lorenz (1955). No other definition is allowed, and the use of a constant temperature T_r makes the theory incompatible with that of Lorenz and weakens the theoretical basis for present formulations of the norm for temperature.

All temperature, pressure and water vapor components of existing squared norms correspond to the quadratic terms $(T')^2$, $(p_s')^2$ or $[\ln(p_s)']^2$ and $(q_v')^2$. It is thus tempting to consider these components as forming a "total energy" squared norm. However, it is explained in Errico (2000) that these squared norms are not based on clear thermodynamic definitions nor on any obvious energy norm of pressure or moisture ("*Although it is called a measure of the energy, it has not been demonstrated that it is indeed such in the contexts to which it has been applied. The fact that it has units of energy per unit mass does not by itself qualify it as a measure of energy*"). Moreover, the moist-air generalization of the APE by Lorenz (1978, 1979) does not lead to any easy-to-use analytical formulation which could replace $\overline{(T')^2}/(2\,\overline{\Gamma})$ with a moist-air version for $\overline{\Gamma}$. This means that the APE approach can not be easily generalized to moist air.

Therefore, other ideas had to be tested in order to solve the problems described so far. Since the temperature component (2) is presently derived from an approximate version of the APE of Lorenz, which was improved by Pearce (1978) and Marquet (1991) for the dry air, and then by Marquet (1993, hereafter M93) for the moist air, this article examines the possibility of deriving the quadratic terms in temperature, pressure and water content from a general principle based on the concept of "moist available enthalpy" defined in M93.

The available enthalpy is one form of what is known as "exergy" in general thermodynamics. This new ex-

ergy norm is used in Borderies et al. (2019) to measure the relative impact of the assimilation of observations on the analysis and short-term forecasts for the French AROME model, with a large impact of the new water-content quadratic term. Indeed, the weighting factors of the exergy norm are significantly different from those used up to now in dry and moist squared norms, in particular by several orders of magnitude for the water content.

In order to achieve some numerical validation of the theoretical formulations for the exergy norm, the same comparisons of the squared norms with inverse analysis increment estimates are made as in MB07.

The motivations for these comparisons can be found in Errico et al. (2004), where a moist norm was used with weights "proportional to estimates of the variances of analysis uncertainty". It was also explained in Barkmeijer et al. (2001) that "in the case of forecast-error covariance prediction, a norm at initial time based on the analysis-error covariance matrix is the more appropriate" (Ehrendorfer and Tribbia, 1997; Palmer et al., 1998; Barkmeijer et al., 1998). At that time, "the analysis-error covariance metric became the reciprocal of the total-energy metric currently used at ECMWF to compute singular vectors for the EPS" (Barkmeijer et al., 1998). And "a specific-humidity norm based on error variances" was experimented by Derber and Bouttier (1999) at ECMWF, leading to a specific-humidity norm defined in Barkmeijer et al. (2001) from the ECMWF "averaged error variances for q_v", with a strong decrease of this norm above 500 hPa, a property that has remained unexplained until now.

This paper is organized as follows. Existing moist-air squared norms are recalled in section 2.1. Section 2.2 presents some theoretical motivations for the use of exergy functions based on the concepts of relative entropy and Kullback-Leibler divergence. The derivations of the moist-air available-enthalpy are conducted in Appendix B to G and the corresponding quadratic approximate squared norm components are shown in section 2.3 for temperature, pressure and water. The datasets from the Canadian Meteorological Centre (CMC), the NASA Goddard Earth Observing System (GEOS) and the French ARPEGE models are described in section 3. These datasets are used to compare the norm components for water and temperature with the Root Mean Square (RMS) of analysis increments, with cross-sections and vertical profiles shown in section 4.1 to 4.3 for the three models, leading to an explanation of the decrease with height of the water vapor exergy terms described in section 4.4. Forecast observation impacts are described in section 4.5 for the GEOS model. Conclusions are drawn in section 5.

2 Theoretical considerations.

2.1 Existing moist-air energy norms.

A moist squared norm is defined in E99 by

$$
N_{\mathrm{E99}} = \iiint \frac{(u')^2 + (v')^2}{2} \frac{dm}{\Sigma} + \iint \frac{R_d\, T_r}{g\, p_r} \frac{(p_s')^2}{2} \frac{d\Sigma}{\Sigma}
$$
$$
+ \iiint \frac{c_{pd}}{T_r} \frac{(T')^2}{2} \frac{dm}{\Sigma}
$$
$$
+ \iiint \frac{w_q(z)\,(L_v)^2}{c_{pd}\, T_r} \frac{(q_v')^2}{2} \frac{dm}{\Sigma}\ . \tag{3}
$$

The state vector is represented by the local departure from mean values of basic quantities, denoted by u', v', T', p_s' and q_v'. The differential mass $dm = \rho\, d\tau$ is equal to $dp\, d\Sigma/g$, where Σ is the horizontal surface area. The volume integrals over dm/Σ and the surface integral over $d\Sigma/\Sigma$ represent energies per unit of horizontal area, all expressed in units of J m^{-2}. The pressure component is expressed in E99 as a volume integral of $R_d\, T_r\, (p_s')^2/(2\, p_r^2)$, but the expressions are equivalent providing that $\overline{p_s} \approx p_r$.

The surface pressure contribution of the squared norm is often expressed differently, in terms of the logarithm of surface pressure, leading to

$$
\iint \frac{R_d\, T_r\, p_r}{g} \frac{[\,\{\ln(p_s)\,\}'\,]^2}{2} \frac{d\Sigma}{\Sigma}\ . \tag{4}
$$

This formalism is retained in C87, Thépaut and Courtier (1991), Buizza et al. (1993), Buizza and Palmer (1995), Rabier et al. (1996), Palmer et al. (1998), Errico (2000).

The two formalisms using the surface pressure or its logarithm are nearly equivalent, providing that $\overline{p_s} \approx p_r$. Indeed, the departure term must be computed as $\{\ln(p_s)\,\}' = \ln(p_s) - \overline{\ln(p_s)}$ in (4) and the perturbation of pressure is equal to $p_s' = p_s - \overline{p_s}$ in (3), leading to $\{\ln(p_s)\,\}' = \ln(1 + p_s'/\overline{p_s}) - \overline{\ln(1 + p_s'/\overline{p_s})} \approx p_s'/\overline{p_s}$ up to small higher order terms.

The justification for the last integral of (3) depending on the variance of water vapor content can be found in Ehrendorfer et al. (1995), Buizza et al. (1996), Mahfouf et al. (1996) and E99. The water contribution

of the squared norm is derived from the temperature contribution $c_{pd}\,(T')^2/(2\,T_r)$ with the additional hypothesis that changes of temperature and moisture are related by $c_{pd}\,T' \approx -L_v\,q'_v$, namely by assuming a conservation of the moist static energy $c_{pd}\,T + L_v\,q_v + \phi$ at constant height for all moist (condensation) process. A similar quadratic term was suggested in C87, where two scale factors for height (H_r) and water content (Q_r) were defined, leading to the equivalent formulation $g\,H_r\,(q'_v)^2\,/\,(Q_r)^2$.

The question addressed in E99 is the relevance of that special formulation for the water contribution. Due to the uncertainty in the assumption $c_{pd}\,T' + L_v\,q'_v \approx 0$ (particularly in frequently under-saturated moist areas without condensation processes), an additional relative weight $w_q(z)$ (also denoted by w^2 or ϵ, depending on papers) is added in the last integral of (3). The effects of making this relative weight larger or smaller than the standard value 1 are discussed in E99 and Barkmeijer et al. (2001), where $w_q(z)$ may increase with height in the upper troposphere and in the stratosphere.

An alternative definition of the water contribution of the squared norm is proposed in MB07 by replacing the assumption of conservation of perturbed moist static energy by a conservation of relative humidity approximated by q_v/q_{sw}. This assumption is expected to be realistic in cloudy areas where relative humidity reaches 100 %, however it may not be realistic in frequently under-saturated moist areas. The constraint of zero departure (at constant pressure) in the quantity $q_v/q_{sw}(T,p)$ corresponds to $q'_v = (\overline{\Gamma}_q)\,T'$, where $\overline{\Gamma}_q = \overline{q_v}\;\partial \ln(\overline{q_{sw}})/\partial\,T$. The alternative contribution proposed in MB07 can be written as

$$\iiint \frac{c_{pd}}{T_r}\,\frac{1}{(\overline{\Gamma}_q)^2}\,\frac{(q'_v)^2}{2}\,\frac{dm}{\Sigma}\,. \qquad (5)$$

MB07 found that this revised formulation for the water component of the norm better match the RMS of the analysis increments than the E99 norm. Indeed, the MB07 formulation better reflects the typical size of perturbations produced by data assimilation systems and (5) accounts for the exponential decrease of specific humidity with altitude, leading to much smaller absolute errors than with the original constant contribution in the last integral of (3). This result agrees with the increase of $w_q(z)$ with altitude considered in Zadra et al. (2004) in moist singular vector computations. The aim was to suppress the impact of humidity perturbations in the stratosphere according to

the results of Buizza et al. (1996) and E99, who showed that for increasing w_q the contribution of the dry fields dominates initially, whereas the contribution of moisture dominates at the final time (and vice versa when w_q is smaller).

According to Errico et al. (2004) and MB07, the grid-point discretization of either (3) or (5) can be written as the inverse variance weighted squared norm

$$\sum_{ijk} \left(\frac{(u'_{ijk})^2}{V_u} + \frac{(v'_{ijk})^2}{V_v} + \frac{(T'_{ijk})^2}{(V_{T1})_{jk}} \right) \omega_{ij}\,\Delta\sigma_k +$$
$$\sum_{ij} \left(\frac{(p'_s)^2_{ijk}}{(V_{p1})_{jk}} \right) \omega_{ij} \; + \; \sum_{ijk} \left(\frac{(q'_v)^2_{ijk}}{(V_{q1})_{jk}} \right) \omega_{ij}\,\Delta\sigma_k\,, \quad (6)$$

where $\Delta\sigma_k$ is the thickness of the layer k in the σ vertical coordinate and ω_{ij} is the fractional coverage of the model grid box defined by the zonal (i) and meridional (j) indices.

The weighting factors V_u, V_v, $(V_{T1})_{jk}$, $(V_{p1})_j$ and $(V_{q1})_{jk}$ will hereafter be referred to as "V-terms". They are interpreted as variances of analysis errors in Errico et al. (2004) and MB07. The indices j and k mean that temperature, surface pressure and water variances can a priori depend on latitude (j) and/or altitude (k).

From (3) and (6), the V-terms in E99 can be written as

$$V_u = V_v = 2 = V_0\,, \quad V_{T1} = V_0\,\frac{T_r}{c_{pd}} = V_0\,\frac{(T_r)^2}{c_{pd}\,T_r}\,, \quad (7)$$
$$V_{p1} = V_0\,\frac{(p_r)^2}{R_d\,T_r}\,,\,(V_{q1})_k = \frac{V_0}{w_q(z)}\,\frac{c_{pd}\,T_r}{(L_v\,Q_r)^2}\,(Q_r)^2. \quad (8)$$

The four terms V_u, V_v, V_{T1} and V_{p1} are all constant, whereas $(V_{q1})_k$ may depend on altitude for water, via the arbitrary weight $w_q(z)$.

All terms in parentheses in (6) are dimensionless in Errico et al. (2004) and MB07, where the dimensions of the square root of $(V_{T1})_{jk}$, $(V_{p1})_j$ and $(V_{q1})_{jk}$ are K, hPa and kg kg^{-1}, respectively. The square-root of these V-terms will be called "SqV-terms" hereafter. The dimensionless characteristic of (6) can be explained by first multiplying all terms of (3) by the dimensionless value 2, and then by dividing all terms by the same energy term $V_0 = 2$ J kg^{-1}. Therefore, the dimensions of $c_{pd}\,T_r$, $R_d\,T_r$ and $L_v\,Q_r$ are same as the one of $V_u = V_v = V_0$, namely in units of m^2 s^{-2} or J kg^{-1}. The value of the dummy specific content Q_r

4

has no impact in (8); it is introduced to highlight the relevant dimension of $kg^2 \, kg^{-2}$ for $(V_{q1})_{jk}$.

The definition (5) proposed by MB07 corresponds to

$$(V_{q2})_{jk} = V_0 \; \frac{T_r}{c_{pd} \, (\overline{T})^2} \; \left(\frac{\overline{T}}{\overline{q_{sw}}} \frac{\partial \overline{q_{sw}}}{\partial T} \right)^2 (\overline{q_v})^2 \;, \quad (9)$$

$$(V_{q2})_{jk} \approx V_0 \; \frac{T_r}{c_{pd}} \; \left(\frac{L_v \, \overline{q_v}}{R_v \, (\overline{T})^2} \right)^2 . \quad (10)$$

From (9), $(V_{q2})_{jk}$ is expressed in $kg^2 \, kg^{-2}$, because $c_{pd} \, (\overline{T})^2 / T_r$ has the same dimension as V_0. This means that the dimension of the square root of $(V_{q2})_{jk}$ is the same as the specific content $\overline{q_v}$, which is expressed in $kg \, kg^{-1}$ and, from (10), varies with altitude via the ratio of the average terms $\overline{q_v}$ and $(\overline{T})^2$.

2.2 Relative entropy, Exergy and Available enthalpy.

Due to the uncertainty and plurality in V_{T1}, V_{q1} or V_{q2} defined in E99 or MB07, and due to the arbitrary values for $w_q(z)$, it is necessary to find a more general and comprehensive "measure," "norm" or "distance" between a perturbed thermodynamic state defined by (T_2, q_{v2}, p_{s2}) and a reference one defined by (T_1, q_{v1}, p_{s1}).

It is explained in section 3 of Marquet and Dauhut (2018) that this distance can be measured by the quantity referred to as "relative entropy" by Shannon (1948) and then defined in Kullback and Leibler (1951) and Kullback (1959) by

$$K(x||y) = \sum_{j=1}^{n} x_j \, \log(x_j/y_j) \quad (11)$$

where the x_j's represent a real state (x) and the y_j's a reference state (y) of the system (see Cover and Thomas, 1991).[1]

This Kullback-Leibler divergence K is usually interpreted as being a non-symmetric measure of how much the x_j's deviate from the y_j's. It also represents the "gain in information" of the state characterized by the distribution (x_j) with respect to the equilibrium distribution (y_j). Therefore, it is unclear whether K corresponds to the measure or the distance between the two thermodynamic states (T_2, q_{v2}, p_{s2}) and (T_1, q_{v1}, p_{s1}).

---

[1] The original notations of Shannon and Kullback using $p(p_j)$ and $q(q_j)$ are replaced here to avoid confusion with the pressure p and the specific water content quantities q_t, q_v, q_l, q_i.

The main difficulty lies in determining the x_j's and the y_j's that correspond to these two thermodynamic states. Moreover, the relative entropy K is clearly different from the entropy $s(x) = -\sum_{j=1}^{n} x_j \, \log(x_j)$ of Shannon (1948), with a change of sign and another reference state y_j included in (11). However, it is possible to show that the macroscopic value of K roughly corresponds to the free energy function $e_i - T_r s$, which is different from the entropy s because it depends on the internal energy e_i and a reference temperature T_r. More precisely, it is shown for instance in Procaccia and Levine (1976), Eriksson and Lindgren (1987) and Karlsson (1990) that the exergy of moist air can be computed by the "available energy" function $a_e = k_B \, T_r \, K$, with $K(x||y)$ given by (11). This function a_e can be written in terms of the local atmospheric variables (p, T, q_n), leading to

$$\begin{aligned} a_e &= (e_i - e_{ir}) + p_r \, (\alpha - \alpha_r) - T_r \, (s - s_r) \\ &\quad - \sum_n \mu_{rn} \, (q_n - q_{rn}) \,, \end{aligned} \quad (12)$$

where the subscript "r" denotes a reference state and where the sum over "n" represents the dry air, water vapor, liquid water and ice species. The specific volume is $\alpha = 1/\rho$ and the specific contents q_n are multiplied by the reference Gibbs functions $\mu_{rn} = h_{rn} - T_r \, s_{rn}$. The quantity a_e given by (12) is called "*maximum available work from a nonflow system*" by Bejan (2016, Eq.5.12) for system at rest reaching a pressure equilibrium with the environment (the laboratory). The last sum over n in (12) is called "*chemical exergy*" by Bejan, while the other terms form the "*nonflow exergy.*"

The sum of the terms $(e_i - e_{ir})$ and $- p_r \, (\alpha - \alpha_r)$ in (12) must be replaced by the difference in specific enthalpy $(h - h_r)$ to form the "*thermomechanical and chemical flow exergy*" defined in Bejan (2016, Eq.5.25). It is the sameavailable enthalpy function as that studied in Marquet (1991) and M93 and corresponding to (B-1), with all other terms of (12) remaining the same, leading to

$$a_m = (h - h_r) - T_r \, (s - s_r) - \sum_n \mu_{rn} \, (q_n - q_{rn}) . \quad (13)$$

The use of the specific enthalpy h to replace the internal energy is motivated by the natural application of h to the flowing moist-air atmosphere. No hypothesis is made from this point of view, since the use of enthalpy does not impose movements that would be

made "at constant pressure". The change in the variable $h = e_i + p/\rho$ is simply mathematical, with no underlying physical assumptions. One of the interests of the introduction of the enthalpy h is the existence of the Bernoulli function $h + g\,z + (u^2 + v^2)/2$, which is constant during stationary, adiabatic and frictionless motions, with a similar Bernoulli's law derived in M93 for $a_m + g\,z + (u^2 + v^2)/2$.

The flow exergy a_m given by (13) ensures the definition of the aforementioned general distance between a perturbed atmospheric state and a reference one. Indeed, since the available enthalpy is the maximum work (or energy) that a system can deliver when passing from a reference state to the real state, this work is produced by transformations from different forms of energy to other forms of energy.

In particular, it is shown in M93 that a Bernoulli equation exists and that the sum $a_m(T, p, q_v, q_l, q_i) + (u^2 + v^2)/2 + \phi$ is conserved along any streamline of an adiabatic frictionless and reversible steady flow of a closed parcel of moist air. This means that the conversions between the potential energy, the kinetic energy and the temperature, pressure and water components of $a_m(T, p, q_v, q_l, q_i)$ given by (13) can be evaluated with the weighting factors V_T, V_p and V_q, ensuring relevant thermodynamic transformations of energy from one form to another.

2.3 The new moist-air available-enthalpy norm.

The three components of the squared norm based on the M93 exergy function given by (13) are derived in the Appendices B to G. They can be written in terms of the square of the perturbations of temperature (G-4), surface pressure (G-11)-(G-13) and water vapor (G-18), leading to

$$N_T = \iiint \left[\frac{c_{pd}\,T_r}{(\overline{T})^2} \right] \frac{(T')^2}{2} \frac{dm}{\Sigma} \ , \tag{14}$$

$$N_p = \frac{R_d\,T_r}{g\,\overline{p_s}} \frac{\overline{(p_s')^2}}{2} = \iiint \left[\frac{R_d\,T_r}{(\overline{p_s})^2} \right] \frac{(p_s')^2}{2} \frac{dm}{\Sigma} \ , \tag{15}$$

$$N_v = \iiint \left[\frac{R_d\,T_r}{(r_0\,\overline{r_v})} \right] \frac{(r_v')^2}{2} \frac{dm}{\Sigma} \ . \tag{16}$$

The new V-terms corresponding to (7)-(10) for temperature, pressure and water content can be written as

$$(V_T)_{jk} = \frac{V_0\,T_r}{c_{pd}} \left(\frac{\overline{T}}{T_r} \right)^2 , \ (V_p)_j = \frac{V_0\,p_r^2}{R_d\,T_r} \left(\frac{\overline{p_s}}{p_r} \right)^2 , \tag{17}$$

$$(V_q)_{jk} = \frac{V_0\,r_0\,\overline{r_v}}{R_d\,T_r} = \frac{p_r - e_r}{e_r} \frac{V_0\,r_r\,\overline{r_v}}{R_d\,T_r} = \frac{V_0\,\overline{r_v}}{R_v\,T_r} \ . \tag{18}$$

From the first formulation in (18), $(V_q)_{jk}$ is independent of r_r. The last formulation in (18) is obtained with $R_v = R_d/r_0$ and $r_0 = r_r(p_r - e_r)/e_r \approx 622 \text{ g kg}^{-1}$, where r_0 is proportional to the reference mixing ratio r_r. This shows that the dimensions of $(V_q)_{jk}$ and of $r_r\,\overline{r_v}$ are both $\text{kg}^2\,\text{kg}^{-2}$, since $V_0 = 2 \text{ m}^2\,\text{s}^{-2}$ and $R_d\,T_r$ have the same dimension. Therefore, the square root of $(V_q)_{jk}$ has the dimension of a mixing ratio, as expected.

From (8) and (17) the pressure V-terms V_{p1} and $(V_p)_j$ may be close to each other if $p_r \approx \overline{p_s} \approx 1000$ hPa, with $(V_p)_j$ only depending on $\overline{p_s}$ and being independent on p_r.

Differently, the temperature and water V-terms can differ significantly because $\overline{T}$ and $\overline{r_v}$ vary with height. This is especially true for $(V_q)_{jk}$ since $\overline{r_v}$ may vary by 3 orders of magnitude from the surface to the stratosphere.

The comparison of (18) with (8) allows a computation of the unknown dimensionless weighting factor $w_q(z)$ in E99, leading to

$$w_q(z) = \frac{c_{pd}\,R_v\,(T_r)^2}{(L_v)^2} \frac{1}{\overline{r_v}(z)} \ , \tag{19}$$

$$w_q(z) = \frac{(c_{pd}\,T_r)\,(R_d\,T_r)}{(L_v\,r_r)^2} \left(\frac{e_r}{p_r - e_r} \right) \frac{r_r}{\overline{r_v}(z)} \ , \tag{20}$$

where $R_v = (R_d\,e_r)/[\,(p_r - e_r)\,r_r\,]$ is used to derive the formulation (20), which better shows the dimensionless feature due to the compensation of the terms $c_{pd}T_r$ and $R_d\,T_r$ with $L_v\,r_r$, also of e_r with $p_r - e_r$ and of r_r with r_v.

The exergy weighting factor (20) explains the expected behavior for $w_q(z)$, which increases with height for decreasing values of $\overline{r_v}(z)$. A similar decrease holds with the MB07 value derived from the comparison of the constant relative humidity V-term (10) with the constant MSE V-term (8), leading to

$$w_{q2}(z) \approx \frac{(c_{pd}\,T_r)^2\,(R_d\,T_r)^2}{(L_v\,r_r)^4} \left(\frac{e_r}{p_r - e_r} \right)^2 \left(\frac{r_r}{\overline{q_v}(z)} \right)^2 . \tag{21}$$

A comparison of (21) with (20) shows that $w_{q2} \approx (w_q)^2$ because $\overline{r_v} \approx \overline{q_v}$. Therefore, the MB07 value is approximately the square of the available enthalpy value,
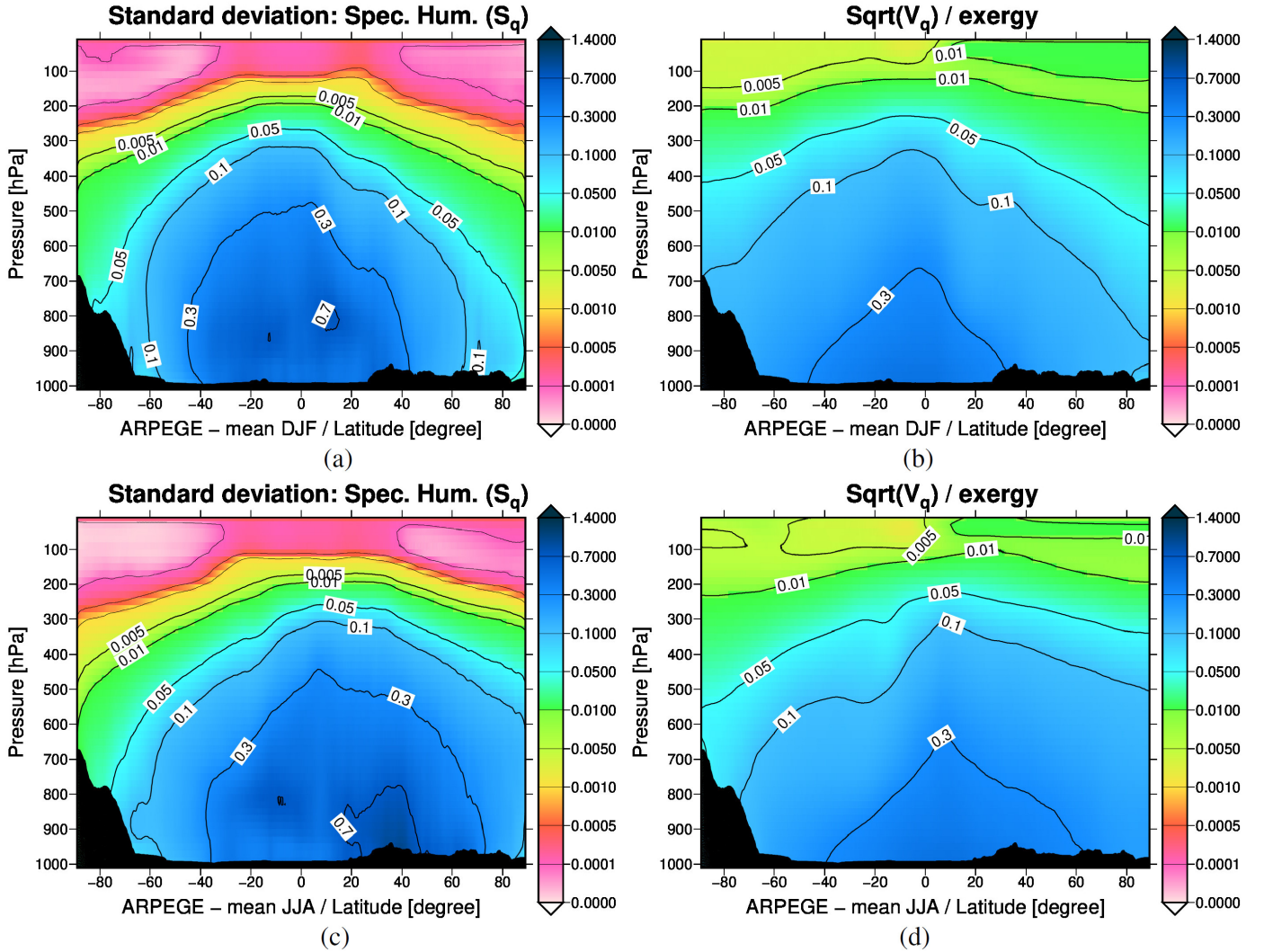
Figure 1: *The seasonal averages of the RMS of analysis increments for water S_q (g kg^{-1}) are computed for ARPEGE outputs every 6 hours and plotted in latitude-pressure sections for: (a) winter (DJF); and (c) summer (JJA). The corresponding seasonal averages of the exergy SqV-term $\sqrt{V_q}$ given by (18) are plotted for: (b) winter (DJF); and (d) summer (JJA).*

leading to an enhanced variation of $w_{q2}(z)$ with height in MB07.

Although the reference value of water content has no impact on the water term $(V_q)_{jk}$ given by (18), it is possible to compute, for the sake of internal consistency and realism, both e_r and r_r for several of the values of T_r and p_r which, from Table 1, are typically used in atmospheric research (semi-implicit algorithms, computation of singular vectors and studies of sensitivity to observations or forecast errors). The result is shown in Table 2 for saturating pressures $e_r = e_{sw}(T_r)$ or $e_{si}(T_r)$ with respect to the more stable state (liquid water or ice), depending on the temperature T_r. The zero Celsius and 280 K temperatures are added to show the rapid increase of both e_r and r_r with T_r for an increase

of a few degrees between 270 and 280 K. The higher temperature $T_r = 350$ K leads to unrealistically large values of r_r, which are even undefined (negative) for 367.8 hPa. The explanation for these impossible values for some couple (T_r, p_r) comes from the fact that e_r is defined as the saturation pressure at the temperature T_r. We therefore assume that $p_r > e_r$, which is not verified for example for $T_r = 350$ K for which $e_r = 411$ hPa is greater than 367.8 hPa in Table 2. But this assumption $p_r > e_r$ does not limit the validity of the theory, in the same way that the assumption $p > e$ for humid air does not limit the two state equations for dry air and water vapour. Therefore the available enthalpy function and the exergy norm are well-defined for values $T_r < 300$ K for which the ratios $|X_v/Y_v|$ are

7

Table 1: *The reference temperatures T_r (K) and pressures p_r (hPa) used (from the left to the right) in: Pearce (1978) and M93, Buizza et al. (1996) and Mahfouf and Buizza (1996), E99 and Holdaway et al. (2014), Errico et al. (2004) and MB07, Janisková and Cardinali (2017).*

	P78/M93	B96/MB96	E99/H14	E04/MB07	JC17
T_r	251	300	270	300	350
p_r	367.8	800	1000	1000	1000

Table 2: *The reference mixing ratio $r_r(T_r, p_r)$ defined as $r_0\, e_r(T_r)/[\,p_r - e_r(T_r)\,]$ in $g\ kg^{-1}$ and the saturated pressure $e_r(T_r)$ in hPa computed for several reference temperatures T_r in K and pressures p_r in hPa.*

$T_r \downarrow \setminus p_r \rightarrow$	367.8 hPa	800 hPa	1000 hPa	$e_r(T_r)$
251 K	$r_r = 1.42$	$r_r = 0.653$	$r_r = 0.522$	(0.838)
270 K	$r_r = 8.11$	$r_r = 3.69$	$r_r = 2.94$	(4.7)
273.15 K	$r_r = 10.6$	$r_r = 4.81$	$r_r = 3.84$	(6.11)
280 K	$r_r = 17.5$	$r_r = 7.86$	$r_r = 6.26$	(9.9)
300 K	$r_r = 70.6$	$r_r = 29.5$	$r_r = 23.3$	(35.3)
325 K	$r_r = 558$	$r_r = 144$	$r_r = 107$	(134)
350 K	$--$	$r_r = 1928$	$r_r = 769$	(411)

greater than 10 in Table E-1, regardless of the pressure p_r.

3   The Datasets.

The RMS of analysis increments S_q and the SqV-terms are computed for three systems using 3DVAR or 4DVAR algorithms. The periods correspond to either individual days, month or seasonal periods. The aim is to show that the temperature and water components of the exergy norm lead torobust results (i.e. that are valid for a wide range of durations and for different systems).

ARPEGE is the NWP model used at the French weather service at Météo-France (Courtier et al., 1991). The horizontal Gauss grid is based on a Schmidt projection with a spectral truncation T1198 and a stretching factor of 2.2 (i.e. with a varying resolution from 7 km over France to 33 km over the South Pacific). The vertical grid has 105 hybrid levels extending from 10 m to 0.1 hPa. The data assimilation is based on a 6-hourly incremental 4DVAR (Courtier et al., 1994), with increments computed at the truncations T149c1 (135 km) and T399c1 (50 km).

The Global Environment Multiscale (GEM) model (Côté et al., 1998a,b) studied in MB07 is used at the Canadian Meteorological Centre (CMC). The global horizontal grid has a uniform resolution of 1.5 degrees in longitude and latitude. The resolution is variable in the vertical, with 28 σ levels extending from the surface up to 10 hPa. The analysis increments are diagnosed by the CMC 3DVAR system (Gauthier et al., 2007).

The Goddard Earth Observing System version 5 (GEOS-5) is an atmospheric global circulation model developed by the National Aeronautics and Space Administration's (NASA) Global Modeling and Assimilation Office (GMAO). The model is based on the finite volume cubed-sphere (FV3) dynamical core (Putman, 2007). The Modern-Era Retrospective analysis for Research and Applications (MERRA-2) Version 2 (Gelaro et al., 2017) is a global reanalysis produced by GMAO using the GEOS forecast model and gridpoint statistical analysis data assimilation system (Wu et al., 2002; Kleist et al., 2009). The 3D-Var system MERRA-2 produces an analysis every 6 hours from 1980 to the present day. The horizontal resolution of the data assimilation and model is around 50 km, or 0.5 degree. In the vertical, 72 hybrid sigma-pressure levels are used, reaching from the surface to 0.01 hPa. The linearized version of GEOS includes the FV3 dynamical core and a linearization of the relaxed Arakawa-Schubert convection scheme (Holdaway et al., 2014, hereafter H14), single moment cloud scheme (Holdaway et al., 2015) and a simplified boundary layer scheme.

4 The results.

4.1 Seasonal means of ARPEGE: the water norms.

The ARPEGE seasonal averages of RMS of analysis increments S_q and exergy SqV-term $\sqrt{V_q}$ are shown in Fig. 1. The winter and summer averages are computed with data 4 times per day (0, 6, 12, 18 UTC).

The general patterns for S_q and $\sqrt{V_q}$ are roughly similar, with a large vertical decrease with height (from 0.5 to less then 0.005 g kg^{-1}) and seasonal latitude oscillations following the regions of maximum surface temperatures (from -15 degree in DJF to $+15$ degree in JJA).

Values close to the ground are of the same order of magnitude for the analysis increments (≈ 0.7 g kg^{-1}), the exergy term (≈ 0.4 g kg^{-1}) and the E99 term ($\sqrt{V_{q1}} \approx 0.31$ g kg^{-1} or 0.57 g kg^{-1} computed with $T_r = 300$ K and $w_q = 1.0$ or $w_q = 0.3$).

The JJA and DJF seasonal means of the "constant RH" value $\sqrt{V_{q2}}$ derived in MB07 are shown in Fig. 2. The seasonal latitude oscillation is similar to that of S_q and $\sqrt{V_q}$ in Fig. 1. The decrease with height of $\sqrt{V_{q2}}$ is larger than for the exergy norm, due to the property $w_{q2} \approx (w_q)^2$ derived from (20)-(21) leading to values of $\sqrt{V_{q2}}$ smaller than 0.0005 g kg^{-1} in the stratosphere (purple color). These values of $\sqrt{V_{q2}}$ are close to those for the RMS of analysis increments above the level 200 hPa.

Vertical profiles are plotted in Fig. 3 for the horizontal means of the RMS of analysis increment S_q and for the V-terms $\sqrt{V_q}$ (exergy), $\sqrt{V_{q1}}$ (E99) and $\sqrt{V_{q2}}$ (MB07).

Almost the same features are observed for the two seasons and for the three latitude domains. The large decrease with height by at least 3 orders of magnitude for the analysis increments S_q cannot be represented by the E99 constant values $\sqrt{V_{q1}} \approx 0.31$ or 0.57 g kg^{-1} with $w_q = 1.0$ or $w_q = 0.3$, nor for any other constant value for w_q.

The differences between the vertical profiles of the RMS of analysis increments, those for the exergy terms and those for the MB07 term remain small from the surface up to about 200 hPa (less than one order of magnitude). The exergy term $\sqrt{V_q}$ is almost similar to the RMS of analysis increments for the layer 500-250 hPa in the tropical and summer extra-tropical
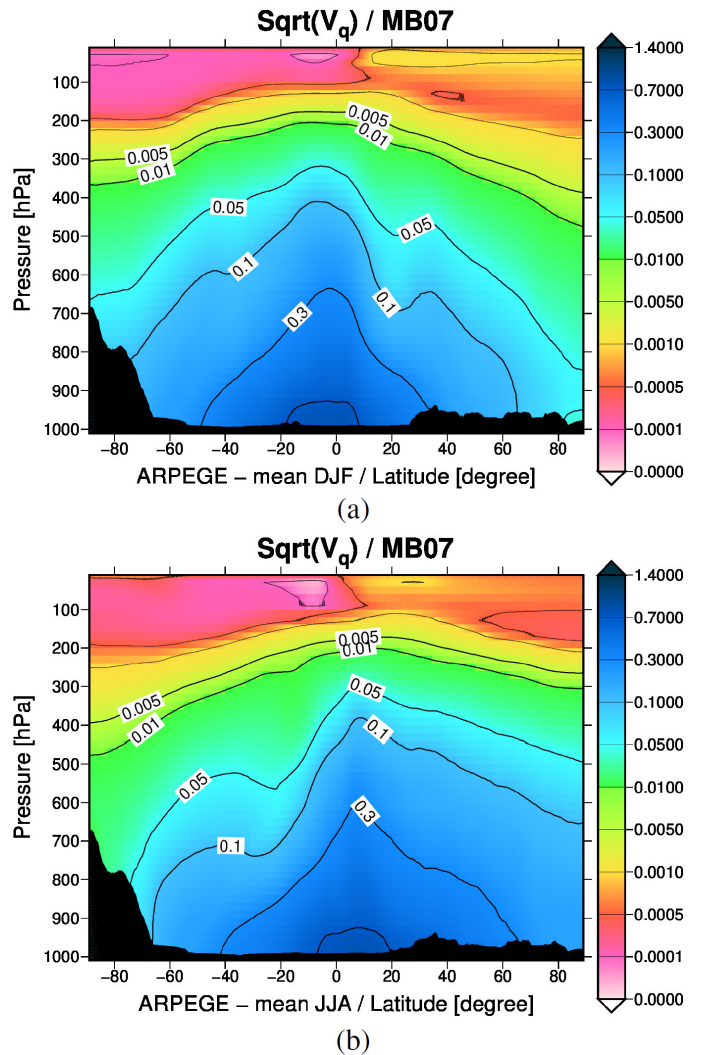

(a)

(b)

Figure 2: *The same as Figs. 1 (b) and (d), but for the DJF and JJA seasonal average of the MB07 water term $\sqrt{V_{q2}}$ given by (9).*

regions, with the blue and red lines intersecting each other. For levels above 100 hPa, the MB07 term is closer to the RMS of analysis increments than the exergy term, with a rapid decrease with height that the exergy term cannot reproduce.

For these reasons, the RMS of the analysis increments, the exergy norm and the MB07 norm are thus similar to each other, while the values for E99 are more different from the other three. The aim was not to perfectly simulate the RMS of the analysis increments, but to approach them qualitatively, both for their vertical variation and for their order of magnitude.

The lack of a contribution from condensed water species to the moist-air exergy norm, together with the absence of any latent heat terms L_v or L_s, may seem
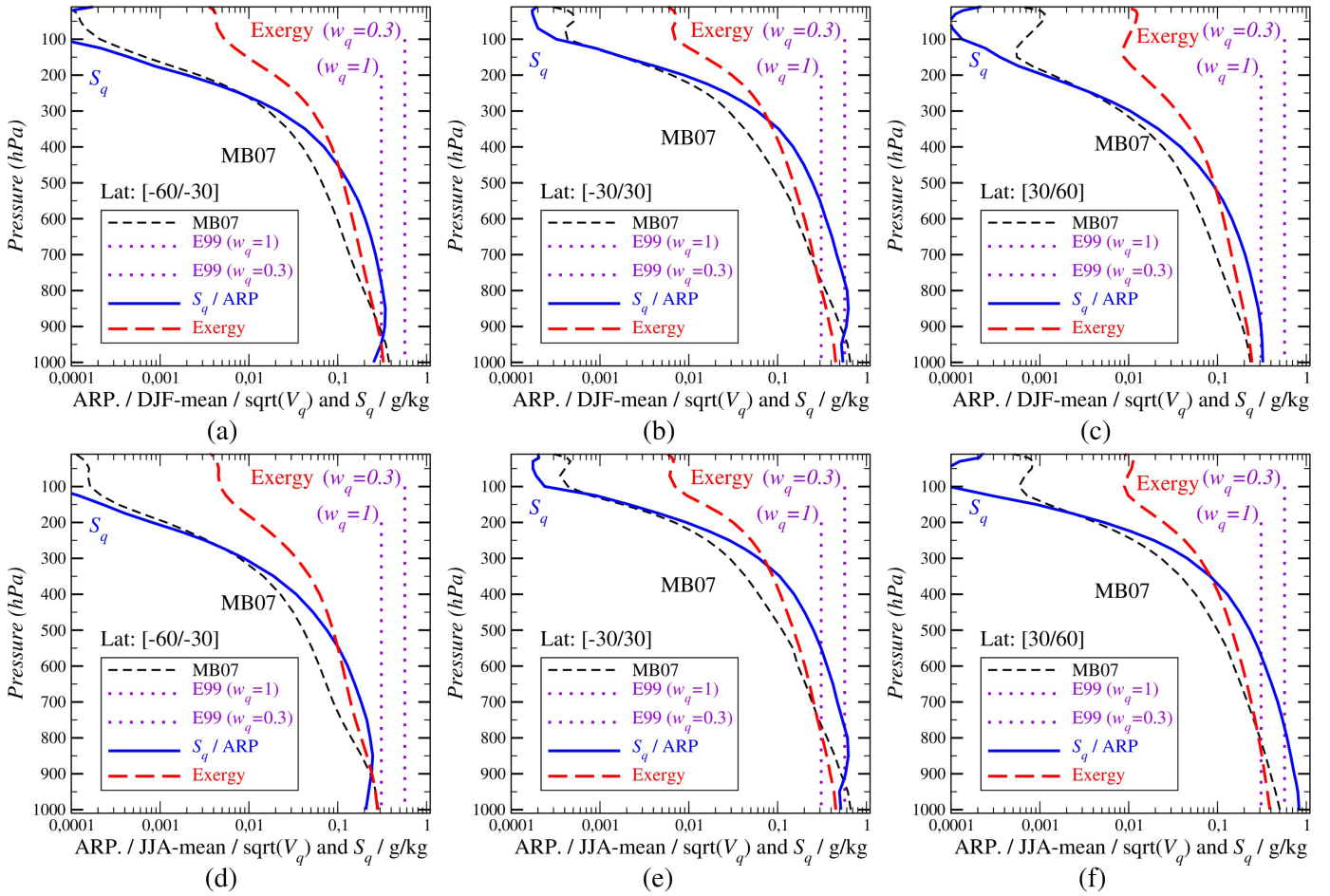
Figure 3: *Vertical profiles of horizontal mean of seasonal averages computed from ARPEGE outputs every 6 hours and for three latitude domains: (a) and (d) southern extra-tropical mid-latitudes from −60 to −30 degrees; (b) and (e) tropical latitudes from −30 to +30 degrees; (c) and (f) northern extra-tropical mid-latitudes from +30 to +60 degrees. The vertical profiles of the DJF means are plotted in (a, b, c); those for the JJA means in (d, e, f). The E99 water terms $\sqrt{V_{q1}}$ (purple dotted lines) are given by (8) with $w_q = 1.0$ and $w_q = 0.3$. The exergy water term $\sqrt{V_q}$ (red dashed lines) is given by (18). The MB07 water term $\sqrt{V_{q2}}$ (black dashed lines) is given by (10). The RMS of analysis increments in water vapor is S_q (blue solid lines).*

surprising. However, the condensed water contents q_l and q_i do exist in (B-1) for the moist-air exergy function a_m, which forms the starting point for deriving the moist exergy squared norm.

It is this theory that ultimately allows q_l and q_i to be neglected in the squared norm components N_T, N_p and N_v, as small correction terms. Moreover, the seasonal averages plotted in Fig. 1 for ARPEGE confirm that there is no need to add independent norms related to the condensates q_l or q_i, because the comparisons between the latitude-section of S_q and $\sqrt{V_q}$ do not reveal missing structures related to the convective regions where q_l and q_i are large (tropical cumulus and extra-tropical frontal regions).

4.2 Seasonal means of ARPEGE: the temperature norms.

The exergy norm seemed able to induce new results, especially for the moisture term $\sqrt{V_q}$ due to the term $\overline{r_v}(p)$ in (18), a result confirmed in the previous section. Similarly, since the ratio $\overline{T}(p)/T_r$ in (17) varies with pressure, and therefore with height, one may wonder whether this variation predicted by the theory is realistic or not.

For this purpose, ARPEGE winter averages of the RMS of analysis increments for temperature S_T and of the temperature exergy term $\sqrt{V_T}$ are shown in Fig. 4. The corresponding vertical profiles of horizontal mean values are plotted in Fig. 5. The summer averages exhibit similar results (not shown).

10

Although the comparisons of norms for each latitude and pressure are less relevant for the temperature components than for the water components (especially within the tropics), the general appearance for S_T and $\sqrt{V_T}$ is approximately similar, with a maximum near the surface (between 1000 and 800 hPa), and a minimum in the tropical troposphere for medium and high levels (between 600 and 100 hPa).

The variations with height of $\sqrt{V_T}$ are similar to those for S_T, while the constant value deduced from the E99 temperature component of the norm ($\sqrt{V_{T1}} \approx$ 0.77 for $T_r = 300$ K) is further from the S_T profile.

Therefore, although variations with height of S_T and $\sqrt{V_T}$ are smaller than those for S_q and $\sqrt{V_q}$, the similarity between the vertical profiles of the seasonal averages of S_T and $\sqrt{V_T}$ confirms the possible crude interpretation of the RMS of analysis increments with the temperature term computed from the squared exergy norm, and with a realistic impact for the ratio $(\overline{T}(p)/T_r)^2$ in (17).

4.3   A specific day for CMC and GEOS systems.

The results presented in the previous sections regarding ARPEGE seasonal averages are encouraging, but the need for daily applications of the exergy norm would require similar variations with height and latitude for a given situation for both the analysis increments and the norms. In addition, the encouraging results obtained with the 4D-Var incremental assimilation of the ARPEGE variable mesh model must be confirmed with different models and/or assimilation schemes.

To do this, the results obtained for the humidity variable are shown in Figs. 6 for one single analysis (26 December 2002, 00 UTC). Outputs from the GEM-CMC system are on the left in (a, c, e) and those from the GEOS-MERRA-2 system are on the right in (b, d, f). The latitude-pressure sections for the RMS of analysis increments S_q in (a, b) are similar to those in Figs.1 (a, b). The vertical profiles of the exergy term $\sqrt{V_q}$, the MB07 term $\sqrt{V_{q2}}$ and the E99 terms $\sqrt{V_{q1}}$ computed with $T_r = 300$ K and $w_q = 1.0$ or $w_q = 0.3$ are similar to those in Figs.3 a.
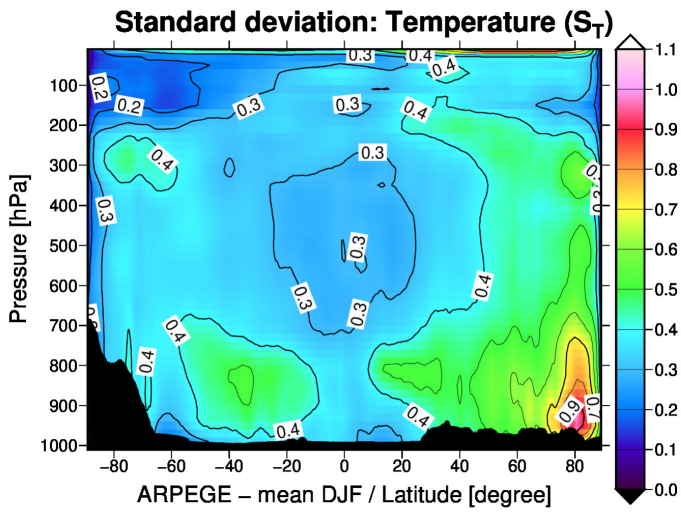
While the RMS of analysis increments are noisier for those GEM-CMC and GEOS-MERRA-2 daily outputs than for the ARPEGE seasonal averages, the same de-

cay with height and relative maxima in the lower layers in the tropics is observed for this particular day. The differences between the three ARPEGE, GEM-CMC and GEOS-MERRA-2 systems are more pronounced above 200 hPa in the upper troposphere and in the stratosphere, where GEM-CMC exhibits larger analysis increments than ARPEGE, while those for GEOS-MERRA-2 are smaller than ARPEGE.

The latitude-pressure sections plotted for the water component of the exergy norm in Figs. 6 (c, d) for GEM-CMC and GEOS-MERRA-2 are similar to those for ARPEGE in Figs.1 (a, b).

The water exergy SqV-term $\sqrt{V_q}$ is relatively smooth and not noisy because it depends on the averaged value of the water vapor $\overline{q_v}$ computed on a circle of latitude, which is less variable in space than the daily RMS of analysis increments S_q.

The results presented in this section for a specific day and for two different systems are therefore broadly comparable to those shown for the ARPEGE seasonal averages. We can therefore be confident that the results derived in this paper from the exergy norm will be robust for other systems with similar patterns of analysis fields.

(a)
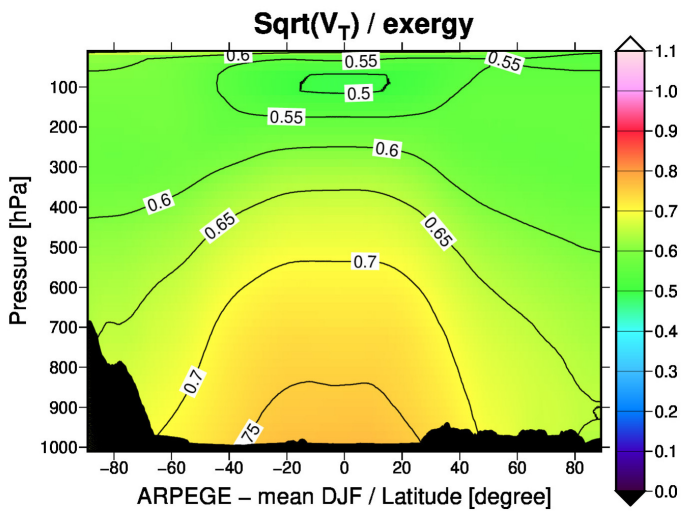
(b)

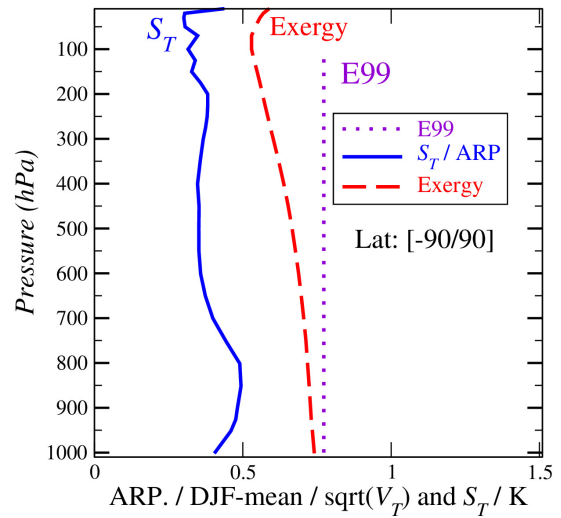Figure 4: *The same as Figs. 1a and 1b, but for temperature (K).*

Figure 5: *The same ARPEGE seasonal mean (DJF) as in Figs. 3a but for temperature (K) and for the RMS of analysis increments S_T (solid blue), the E99 term $\sqrt{V_{T1}} \approx 0.77$ (dotted purple) and the exergy term $\sqrt{V_T}$ (red dashed).*
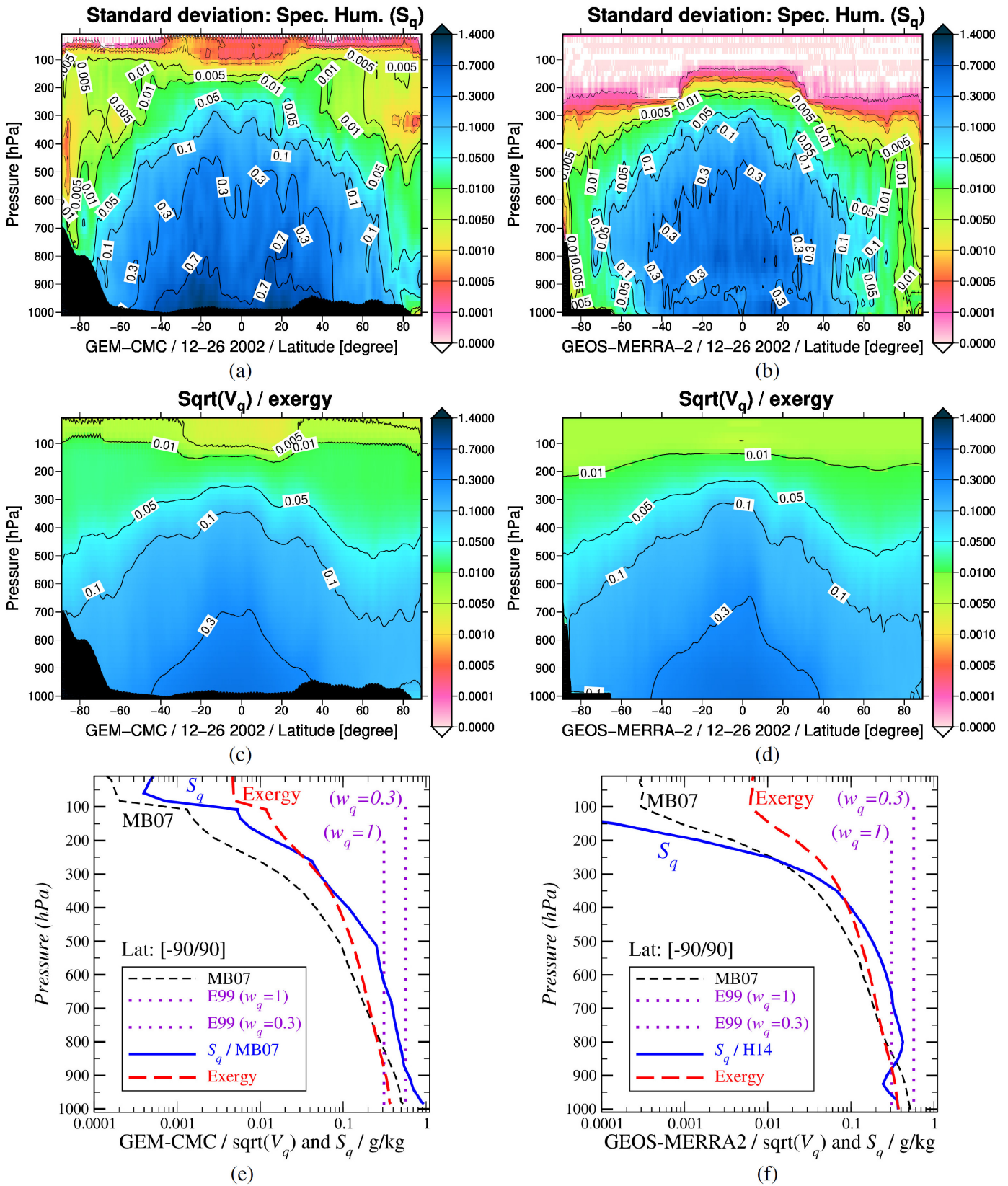
Figure 6: *Latitude-pressure sections and vertical profiles of horizontal averages for the water term for the 26th of December 2002: in the left panels (a, c, e) for the GEM-CMC; in the right panels (b, d, f) for GEOS-MERRA-2. At the top (a, b): sections of the RMS of analysis increments S_q (g kg^{-1}). On the center (c, d): sections of exergy norms $\sqrt{V_q}$ (g kg^{-1}). At the bottom (e, f): vertical profiles of horizontal averages of E99 (dotted purple), MB07 (dashed black) and Exergy (dashed red) norms and the analysis increments S_q (solid blue).*
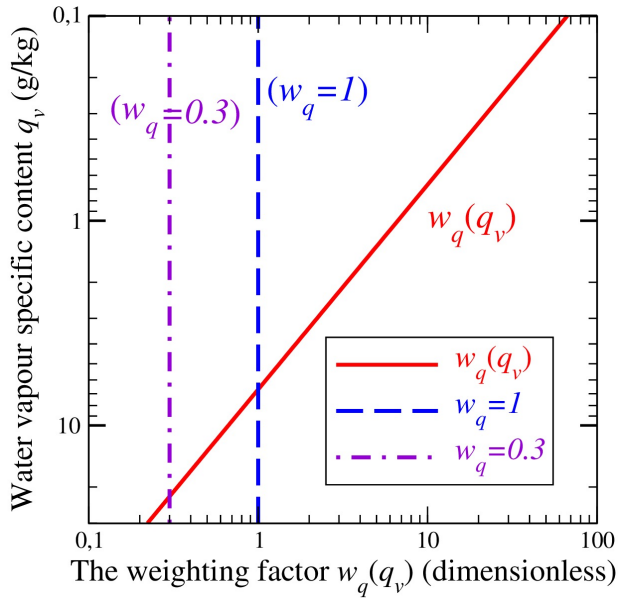
13

Figure 7: *The dimensionless exergy weighting factor $w_q(q_v)$ given by (19) plotted with q_v in ordinates.*
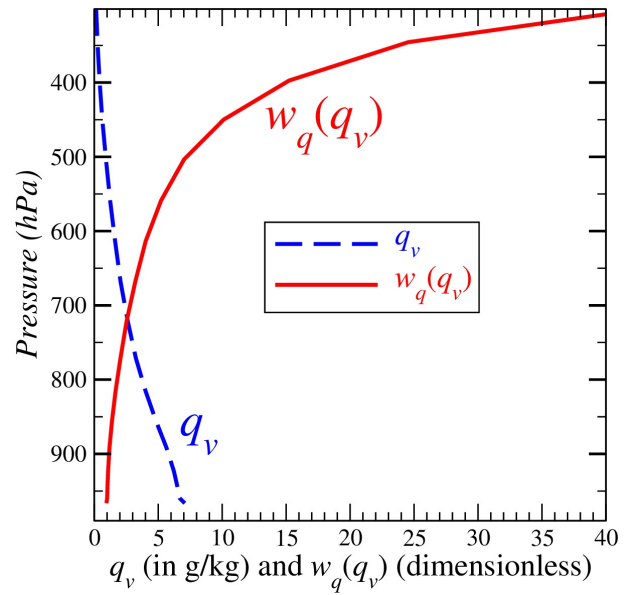

Figure 8: *The dimensionless exergy weighting factor $w_q(z)$ given by (19) for the vertical profile of average values $\overline{q_v}(p)$ of the GEM-CMC dataset used to plot the Fig. 6c.*

14

4.4   The decrease with height of w_q.

The advantage of the exergy approach is that it provides an analytic formulation for the weighting factor w_q given by (19). As an example, values of $w_q(q_v)$ are plotted in Fig. 7 for $0.1 < q_v < 25$ g kg^{-1}.

The weighting factor $w_q(r_v)$ is smaller than unity for moist low levels where $q_v > 6.7$ g kg^{-1} for $T_r = 300$ K, and it is equal to 0.33 for $q_v \approx 20$ g kg^{-1}. Conversely, it is much larger than unity for small values of q_v, reaching $w_q \approx 67$ for $q_v \approx 0.1$ g kg^{-1} in the upper troposphere and $w_q \approx 6700$ for $q_v \approx 0.001$ g kg^{-1} in the stratosphere.

It is also possible to plot the vertical profiles of w_q in terms of the horizontal mean value $\overline{q_v}(p)$ computed from the GEM-CMC simulation, shown in Fig. 8. The large increase of w_q with height, with a factor varying non-linearly from 1 to 40 for the pressure varying from 1000 hPa to 300 hPa, is similar to the one proposed empirically in previous studies; for instance, a weight of $w_q(r_v) \approx 5$ was evaluated for the lower part of the atmosphere in Barkmeijer et al. (2001) from the ECMWF averaged error variances for q_v, with $w_q(r_v)$ strongly increasing above 500 hPa. This description is consistent with the exergy weight displayed in Fig. 8.

The same relation used to plot these diagrams "w_q in terms of q_v" is used to plot the exergy norm in the pressure (p) and latitude (φ) sections shown in Figs. 1 (b and d) and 6 (c and d), where the zonal averages $\overline{q_v}(\varphi, p)$ varies with both pressure and latitude.

4.5   FSOI.

The Forecast Sensitivity to Observation Impact (FSOI) method can be used to assess and compare the capacity of various observing systems to reduce a given short-range forecast error produced by a NWP model, e.g. Baker and Daley (2000), Langland and Baker (2004), Cardinali (2009), Gelaro et al. (2010). Typically, fields from a 24 h forecast are compared against a verifying analysis, in terms of u, v, T, p_s and q_v using an inner product based on the E99 energy norm with different values of w_q in the moist term. The adjoint of the forecast model is used to propagate a sensitivity backwards from verifying time (24 h) to obtain a sensitivity at analysis time (0 h). The adjoint model can include both dry physical processes (turbulent diffusion, radiation, gravity wave drag) and moist processes (large scale condensation, moist convection).

Impacts shown in the present paper are examined in averages per observation system and for the global domain with the E99 norms (7)–(8) where $T_r = 270$ K, $p_r = 1000$ hPa and $w_q = 0.3$. The value of 0.3 is chosen empirically in H14 to produce approximately equal weighting between the temperature and specific humidity components of the norm.

The metrics monitored at GMAO are: impact per analysis, impact per observation, fraction of beneficial observations, and observation count per analysis. The observation impacts are computed as reductions in the final 24 h forecast errors due to any given extra set of observations included in the initial analysis. The adjoint model can be used to propagate the final energy norm gradient backward 24 h in order to obtain sensitivities of these forecast errors at the initial time (Trémolet, 2008). These sensitivities are then passed through the adjoint of the data assimilation system to convert them into observation space and to provide the impacts.
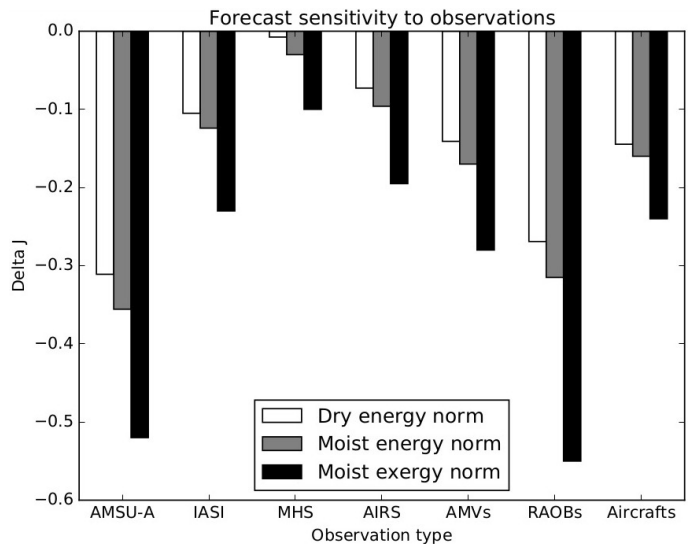
Figure 9: *The 24-h forecast observation impacts per analysis for each observation system. Comparisons of: i) the Dry norm (white); ii) the moist norm E99 with $w_q = 0.3$ (grey), namely the same as Fig. 9 in H14; and iii) the moist exergy norm (dark).*

Fig. 9 compares the 24 h forecast error reductions produced by various observing systems included in the MERRA-2 data assimilation system with three different inner products for the estimation of the global forecast error: the E99 "dry energy squared norm" with $w_q = 0.0$, the E99 "moist energy squared norm" with $w_q = 0.3$, and the "exergy squared norm" $N_T + N_p + N_v$ introduced in Eqs. (14)-(16) of Section 2.3.

Table 3: *The increase in observation impacts (in percentage) corresponding to Fig. 9 for the change of the Dry norms to the moist E99 with $w_q = 0.3$ (first line), and then to the moist Exergy (second line).*

	AMSU-A	IASI	**MHS**	AIRS	AMVs	RAOBs	Aicrafts
100 (E99 / Dry − 1)	14	17	300	32	21	18	10
100 (Exergy / E99 − 1)	47	85	**253**	105	69	74	50

The impacts of the dry energy E99 squared norms are those computed and studied in Fig.9 of H14 for the month 17 March-17 April 2012. The impacts for the two moist squared norms (E99 with $w_q = 0.3$ and exergy formulations) are computed for another month (1-30 September 2015). For convenience, the impacts of the three dry and moist squared norms are compared on the same plot despite having been computed over those two distinct periods. In all experiments, the adjoint model includes a comprehensive set of physical processes with moist processes as described in H14.

As expected from the definition of the moist energy norm, impacts are larger when they include the moist term, as already shown in H14. It is interesting to note that the increase in observation impacts not only holds for observations sensitive to atmospheric water vapor, such as radiosoundings, but also for observation systems where only a small subset of the observations directly measure moisture, such as IASI (Infrared Atmosphere Sounding Interferometer) radiances, AMSU-A (Advanced Microwave Sounding Unit) radiances which are sensitive to atmospheric temperature, and AMVs (Atmospheric Motion Vectors) which are directly sensitive to horizontal wind components. These results show that a reduction of forecast error in the moisture field is possible through observations of temperature and wind. This could occur through dynamical balance, for example.

The ranking, in terms of contributions of the various observing systems to the forecast error reduction, is unchanged when moving from $E99/w_q = 0.0$ to $E99/w_q = 0.3$. Similarly, when examining the impact with the exergy norm instead, it is clear that the overall observation impact is larger, but that the ranking of the observation systems relative to each other is almost the same. Larger values come from the difference in the weighting factor w_q applied to the moisture at upper levels, which does not depend on height for the E99 norm and increases with height for the exergy norm according to Fig. 8.

The most striking feature, when using the exergy norm, is the very large increase by a factor of three

(or $> +200$ %, see Table.3) of the only observing system highly sensitive to atmospheric water vapor: the Microwave Humidity Sounder (MHS). According to Fig. 9, RAOB ranks first for the exergy norm, which may have important implications given that the operational radiosonde observing network is expensive to operate. These results suggest that radiosonde humidity sensors play an important role in the 24 h forecast accuracy, even more than MHS.

5   <u>Conclusions.</u>

The main objective of this paper is to provide a general and more satisfactory method for combining thermodynamic variables of the atmosphere into a norm. There are several formulations for these norms currently in use for a wide variety of important applications, yet until now all have been derived using heuristic methods and approximations.

It is argued in this paper that such approximations can be avoided by instead considering the principles of fundamental physics more carefully. Specifically, the approach is to start with some general exergy functions, which are constructed by combining the first (enthalpy) and second (entropy) law of thermodynamics, leading to the available enthalpy function a_m derived in M93. This kind of exergy function is also based on the concept of relative entropy or Kullback distance, two equivalent concepts which are already used in many papers dealing with assimilation techniques.

The choice of the exergy (available enthalpy) squared norms provides not only the quadratic terms $(T')^2$, $(p'_s)^2$ and $(q'_v)^2$, but also values for the weighting factors which multiply these quadratic terms. It is shown in the present paper that the weighting factors for T and q_v vary with height in the same way as the RMS of analysis increments. This ensures an even weighting of all variables and all levels when computing the global norm. Such results are valid for both seasonal average periods and for a particular day.

The fact that the weights for the exergy norm for

T and q_v are close to the RMS of analysis increments is not straightforward. Indeed, if the observation system is radically changed, the increments could be very different, while the exergy-norm weights would not be modified. To better understand the complex links that can exist between fields as different as thermodynamics, information theory and data assimilation, it is possible to refer to papers cited in section 3 of Marquet and Dauhut (2018).

Inspired by previous studies by Kleeman (2002) and Majda et al. (2002), the paper of Xu (2006) examined the use of the relative entropy or Kullback-Leibler distance $K(x||y)$ given by (11) *"to measure the information content of the pdf produced by an optimal analysis of observations (or compressed super-observations) with respect to a prior background pdf used by the analysis (...) where the background pdf can be always considered as an approximation of the analysis pdf."* Xu showed that the integral form of the relative entropy $K(x||y)$ *"is a quadratic form of the analysis increment vector weighted by B^{-1}"*, and *"yields an explicit formulation in which the signal part is given by the inner-product of the analysis increment vector weighted by the inverse of the background covariance matrix"* (B^{-1}).

Since Xu (2006) demonstrated a close relationship between $K(x||y)$ and the weighting factors V_u, V_v, V_v, V_p, V_T and V_q, the next step is to use the close relationship shown by Procaccia and Levine (1976), Eriksson and Lindgren (1987), Eriksson et al. (1987), Karlsson (1990) and Honerkamp (1998) between $K(x||y)$ and exergy functions, to foresee a direct link between the moist-air exergy defined in thermodynamics and the weighting factors used in data assimilation.

The new exergy (available enthalpy) squared norm may solve the main disadvantage of using the constant E99 moist V-term stated in Rivière et al. (2009), namely that the weight for water is no longer proportional to the weight for temperature with the exergy formulation, leading to new results with the use of the V_q term.

A first usage of the exergy norm in the context of FSOI experiments has shown that it increases observation impact in a way similar to what has previously been described when going from a dry energy norm to a moist energy norm (e.g. H14). However, the enhancement of the impact is larger, since the exergy norm accounts more evenly for moisture forecast errors between the various atmospheric layers, whereas the moist energy norm penalizes the upper tropospheric levels. The results are very similar among the various observing systems, however with a noticeable difference for the MHS and RAOBs, for which the contributions are particularly enhanced with the exergy norm. This is in agreement with the known impact of microwave humidity sounders from direct observing system experiments (Karbou et al., 2010; Chambon et al., 2015). In consequence, it is expected that the various observing systems would be more fairly ranked through more balanced contributions between wind, temperature and water vapor forecast errors through the use of the exergy norm in FSOI experiments.

Another usage of the exergy norm has been shown by Borderies et al. (2019) to demonstrate the impact of airborne cloud radar reflectivity data assimilation.

The important point is that the analytical formulation of the exergy norm is not complicated. It is comparable in complexity to existing formulations (E99, MB07) and can be easily coded and used in operational systems, for moist singular vector and FSOI calculations as well as forecast verifications. The only new aspect is the need to take into account horizontal averages, or averages on each latitude circle, for the mean temperature and vapor content variables $\overline{T}$ and $\overline{r_v}$ that appear in (14)-(18) to define N_T, N_v, V_T and V_q.

Acknowledgements.

Appendix A. List of symbols and acronyms.

B_p — a dummy notation for a pressure norm

APE — the global available potential energy (Lorenz)

α — the specific mass of moist air (the density $1/\rho$)

a_e — the moist specific available energy

a_h, a_m — the dry and moist specific available enthalpies

a_T, a_p — temperature and pressure components of a_h and a_m

a_v — the water component of a_m

c_{pd} — specific heat of dry air (1004.7 J K^{-1} kg^{-1})

c_{pv} — spec. heat of water vapor (1846.1 J K^{-1} kg^{-1})

c_l — spec. heat of liquid water (4218 J K^{-1} kg^{-1})

c_i — spec. heat of ice (2106 J K^{-1} kg^{-1})

c_p — the moist-air spec. heat at constant pressure, $= q_d\, c_{pd} + q_v\, c_{pv} + q_l\, c_l + q_i\, c_i$

δ — $= R_v/R_d - 1 \approx 0.608$

e — the water-vapor partial pressure

e_i — the specific internal energy

e_r — the water-vapor reference partial pressure, with $e_r = e_{sw}(T_r) \approx 6.11$ hPa

F, H — dimensionless functions of X or Y

g — magnitude of Earth's gravity (9.8065 m^2 s^{-2})

$\overline{\Gamma}$ — the Lorenz stability parameter

$\overline{\Gamma}_q$ — a weight in water component of MB07 norm

h, H — specific and global enthalpies

H_r — a dummy scale height (C87)

k_B — the Boltzmann constant

K — Kullback function, contrast, relative entropy

L_f — $= h_l - h_i$: latent heat of melting

L_v — $= h_v - h_l$: latent heat of vaporization

L_s — $= h_v - h_i$: latent heat of sublimation

$L_f(T_r)$ — $= 0.334\ 10^6$ J kg^{-1}

$L_v(T_r)$ — $= 2.501\ 10^6$ J kg^{-1}

$L_s(T_r)$ — $= 2.835\ 10^6$ J kg^{-1}

m — a mass of moist air

dm — the element of mass ($= \rho\, d\tau$)

N — the global available enthalpy squared norms

ω_{ij} — the fractional coverage of the model grid box

x_j, y_j — the micro states which define the function K

p — the pressure ($p = p_d + e$)

p_s — the surface pressure

q — the specific content (ex. $q_v = \rho_v/\rho$)

Q_r — a dummy specific water content (C87)

r — the mixing ratio (ex. $r_v = \rho_v/\rho_d$)

r_0 — $= R_d/R_v \approx 0.622 = 1/1.608$

ρ — specific mass of moist air ($= \rho_d + \rho_v + \rho_l + \rho_i$)

R_d — dry-air gas constant (287.06 J K^{-1} kg^{-1})

R_v — water-vapor gas constant (461.52 J K^{-1} kg^{-1})

R — gas constant for moist air ($= q_d\, R_d + q_v\, R_v$)

s — the specific entropy

σ — the vertical coordinate of the model grid box

$\Sigma, d\Sigma$ — global and element of horizontal surface of Earth

T — the absolute temperature

T_r — the reference zero Celsius temperature (273.15 K)

$\boldsymbol{U}$ — the horizontal wind and its components (u, v)

U — the horizontal wind speed $\sqrt{u^2 + v^2}$

μ — the specific Gibbs' function ($h - T\, s$)

ϕ — the gravitational potential energy ($g\, z + Cste$)

V — the variances of analysis errors

V_0 — a special variance of 2 J kg^{-1}

w_q — a relative weight in water components of norms

Z — a dimensionless water vapor variable

GCM — General Circulation Model

NWP — Numerical Weather Prediction

Lower indices (for h, s, p, μ, ρ, q, r, V, X, Y, Z):

r — reference value (entropy, available enthalpy)

d, v — dry-air and water vapor gases phases

l, i — liquid water and ice condensed phases

sw, si — saturating value (over liquid or ice)

t — total water value (vapor plus liquid plus ice)

T, p, v — temperature, pressure and water components

$T_1, p1$ — notations for pressure components (V)

$q, q2$ — notations for water components (V)

$1, 2$ — notations in separating laws

i, j, k — indices for longitude, latitude and altitude

Upper indices/operator:

$(\ldots)'$ — departure terms from average values

$\overline{(\ldots)}$ — average values

App. B. The specific moist-air available enthalpy.

The specific moist available enthalpy a_m is an exergy function defined in M93 (see Eq. (17), page 574) as a sum of four partial moist available enthalpies for dry air $(a_m)_d$, water vapor $(a_m)_v$, liquid water $(a_m)_l$ and ice $(a_m)_i$, leading to

$$a_m = q_d\,(a_m)_d + q_v\,(a_m)_v + q_l\,(a_m)_l + q_i\,(a_m)_i, \quad \text{(B-1)}$$

$$(a_m)_d = [\, h_d - (h_d)_r\,] - T_r\,[\, s_d - (s_d)_r\,], \quad \text{(B-2)}$$

$$(a_m)_v = [\, h_v - (h_v)_r\,] - T_r\,[\, s_v - (s_v)_r\,], \quad \text{(B-3)}$$

$$(a_m)_l = [\, h_l - (h_l)_r\,] - T_r\,[\, s_l - (s_l)_r\,], \quad \text{(B-4)}$$

$$(a_m)_i = [\, h_i - (h_i)_r\,] - T_r\,[\, s_i - (s_i)_r\,], \quad \text{(B-5)}$$

where T_r is a constant reference pressure.

Differences in enthalpy and in entropy can be computed for dry air, water vapor and condensed species by assuming that the specific heat at constant pressure (c_{pd}, c_{pv}, c_l, c_i) and gas constants (R_d, R_v) are all constant for the atmospheric range of temperature (from 180 to 320 K), leading to

$$h_d - (h_d)_r = c_{pd}\,(T - T_r),\; h_v - (h_v)_r = c_{pv}\,(T - T_r),\; \text{(B-6)}$$
$$h_l - (h_l)_r = c_l\,(T - T_r),\; h_i - (h_i)_r = c_i\,(T - T_r),\quad \text{(B-7)}$$

and

$$s_d - (s_d)_r = c_{pd}\ln(T/T_r) - R_d\ln[\,p_d/(p_d)_r\,]\,,\qquad \text{(B-8)}$$
$$s_v - (s_v)_r = c_{pv}\ln(T/T_r) - R_v\ln[\,e/e_r\,]\,,\qquad \text{(B-9)}$$
$$s_l - (s_l)_r = c_l\ln(T/T_r)\,,\; s_i - (s_i)_r = c_i\ln(T/T_r)\,.\,\text{(B-10)}$$

The reference partial pressure e_r is equal to the ice-vapor value $e_{si}(T_r)$ for $T_r < 0\,°\,$C or to the liquid-vapor value $e_{sw}(T_r)$ for $T_r > 0\,°\,$C. The moist available enthalpy (B-1) is computed by including (B-6)-(B-10) in (B-2)-(B-5), yielding

$$a_m = c_p\left[\,T - T_r - T_r\ln\left(\frac{T}{T_r}\right)\right]$$
$$+\,T_r\left[\,q_d\,R_d\,\ln\left(\frac{p_d}{(p_d)_r}\right) + q_v\,R_v\,\ln\left(\frac{e}{e_r}\right)\right].\;\text{(B-11)}$$

Here q_l and q_i are not neglected, but appear in the moist values of c_p and $q_d = 1 - q_v - q_l - q_i$, anywhere else.

App. C. The temperature component of a_m.

The first term on the R.H.S. of (B-11) is the Motivity defined by Lord Kelvin (Thomson, 1853). It corresponds to the moist temperature component a_T of the available enthalpy defined in Marquet (1991, hereafter M91) and M93 in terms of the function $F(X)$ according to

$$a_T\,(T) = c_p\;T_r\;F(X_T)\,,\quad X_T = T/T_r - 1 > -1\,,$$
$$\text{(C-1)}$$
$$F(X) = X - \ln(1 + X)\,.\qquad\qquad \text{(C-2)}$$

The difference from the dry case studied in M91 is that c_p is equal to $q_d\,c_{pd} + q_v\,c_{pv} + q_l\,c_l + q_i\,c_i$ and is not a constant, since it depends on varying specific contents of dry air and water species.

$F(X)$ is positive and asymmetric with respect to $X = 0$, see Fig. C-1 It is a quadratic-like function because $F(X) \approx X^2/2$ for $|X| < 0.3$. This terminology
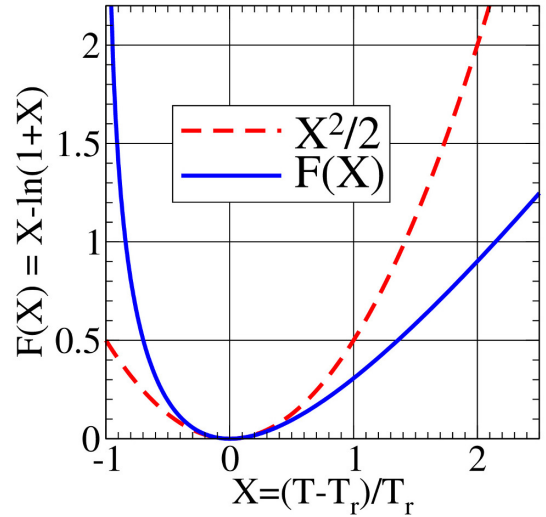

Figure C-1: *The two functions $F(X) = X - \ln(1 + X)$ and $X^2/2$ plotted for $-1 < X < +2.5$.*

"quadratic-like" corresponds to functions with Taylor series of the form: $X^2/2 + a\,X^3 + b\,X^4 + ...$, where the quadratic term $X^2/2$ is the first order approximation and where the other higher-order terms can be discarded. This approximation is typically valid for $210\text{ K} < T < 390\text{ K}$ if $T_r = 300$ K. $F(X) = 0$ only for $X = 0$, namely for $T = T_r$.

Appendix D. The pressure components of a_m.

Terms in the second line of (B-11) can be rearranged in order to compute the separate quadratic contributions due to total pressure $p = p_d + e$ on the one hand, and to water species contents (q_v, q_l or q_i) on the other hand.

The three state functions for moist air, dry air and water vapor can be written as $p = \rho R T$, $p_d = q_d\,\rho\,R_d\,T$ and $e = q_v\,\rho\,R_v\,T$, respectively, leading to

$$T_r\,q_d\,R_d = p_d\,T_r/(\rho\,T) = R\,T_r\,p_d/p\,,\qquad \text{(D-1)}$$
$$T_r\,q_v\,R_v = e\,T_r/(\rho\,T) = R\,T_r\,e/p\,,\qquad \text{(D-2)}$$

where the moist gas constant $R = q_d\,R_d + q_v\,R_v$ is not a constant since it varies with q_d and q_v.

The terms $q_d\,R_d$ and $q_v\,R_v$ given by (D-1) and (D-2) can be inserted into (B-11), yielding

$$a_m = a_T + R\,T_r\left[\frac{p_d}{p}\,\ln\left(\frac{p_d}{(p_d)_r}\right) + \frac{e}{e_r}\,\ln\left(\frac{e}{e_r}\right)\right].\;\text{(D-3)}$$

The next step is to isolate the pressure component a_p defined by (D-4), leading to the separation of a_m into

$$a_m = a_T + a_p + a_v , \quad a_p = R\,T_r\,\ln\!\left(\frac{p}{p_r}\right), \quad \text{(D-4)}$$

$$a_v = R\,T_r\left[\frac{p_d}{p}\,\ln\!\left(\frac{p_d}{p}\,\frac{p_r}{(p_d)_r}\right) + \frac{e}{p}\,\ln\!\left(\frac{e}{p}\,\frac{p_r}{e_r}\right)\right], \quad \text{(D-5)}$$

where the remaining terms grouped in (D-5) form the water components a_v.

It is not possible to define directly a squared norm starting from the term $\ln(p/p_r)$, since it is negative for $p < p_r$. This apparent drawback was already mentioned in M91 and M93. However, it is possible to integrate by parts a_p in (D-4) with respect to p, leading to

$$a_p = R\,T_r\,p_r\,\frac{\partial}{\partial p}\left[\frac{p}{p_r}\,\ln\!\left(\frac{p}{p_r}\right) - \left(\frac{p}{p_r} - C\right)\right]. \quad \text{(D-6)}$$

A new quadratic-like function $H(X)$ can be introduced by choosing the constant of integration $C = 1$, yielding

$$a_p = R\,T_r\,\frac{\partial}{\partial p}\left[\,p_r\,H(X_p)\,\right], \quad X_p = \frac{p}{p_r} - 1, \quad \text{(D-7)}$$

$$H(X) = (1+X)\,\ln(1+X) - X , \quad \text{(D-8)}$$

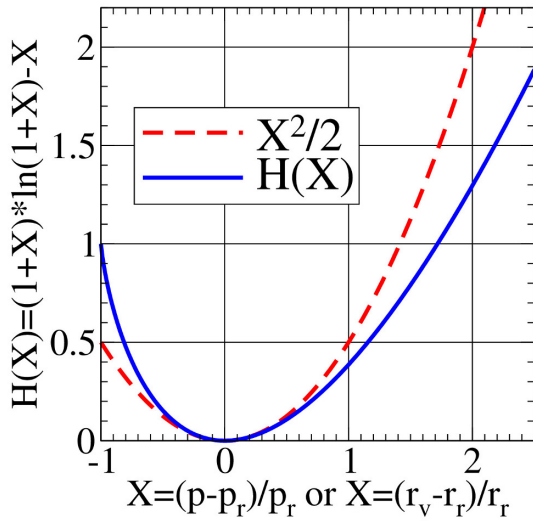where X_p is the dimensionless pressure control variable.

Figure D-1: *The two functions $H(X) = (1+X)\ln(1+X)-X$ and $X^2/2$ plotted for $-1 < X < +2.5$.*

It is shown in Fig. D-1 that $H(X)$ is positive and asymmetric with respect to $X = 0$. It is a quadratic-like function because $H(X) \approx X^2/2$ up to higher order terms. $H(X) = 0$ only for $X = 0$, namely for $p = p_r$.

The constant reference pressure p_r can enter the derivative in (D-7) and the term $p_r\,H(X_p)$ is equal

to the function $p_r - p + p\,\ln(p\,/p_r) \approx (p - p_r)^2/(2\,p_r)$ called "store of work for any layer under isothermal conditions" in Margules (1910) and studied in Eq. (Ia)' page 505, the bottom of page 506 and the top of page 507 of this old paper.

Appendix E. The water components of a_m.

The aim of this section is to show that a_v given by (D-5), which depends on the six pressures p, p_r, p_d,$(p_d)_r$, e and e_r, can be expressed in terms of the sole water mixing ratios $r_v = q_v/q_d$ and r_r. In this way, a_v will be interpreted as the water-vapor component of a_m.

Division of (D-2) by (D-1) leads to $e/p_d = r_v/r_0$, where $r_0 \equiv R_d/R_v = 0.622$. The same result is valid for the reference state, leading to $e_r/(p_d)_r = r_r/r_0$ and to a reference value for the mixing ratio given by

$$r_r = r_0\,e_r\,/\,(p_d)_r . \quad \text{(E-1)}$$

This reference mixing ratio is fully determined if T_r and p_r are known, because $p_r = (p_d)_r + e_r$ and $e_r(T_r)$ is the saturation pressure of water at T_r and $(p_d)_r = p_r - e_r(T_r)$ can then be computed.

The four pressure terms involved in (D-5) are computed by using $e/p_d = r_v/r_0$ and $e_r/(p_d)_r = r_r/r_0$, leading to

$$\frac{p_d}{p} = \frac{p_d}{p_d + e} = \frac{r_0}{r_v + r_0}, \quad \frac{p_r}{(p_d)_r} = \frac{r_r + r_0}{r_0}, \quad \text{(E-2)}$$

$$\frac{e}{p} = \frac{e}{p_d + e} = \frac{r_v}{r_v + r_0}, \quad \frac{p_r}{e_r} = \frac{r_r + r_0}{r_r}. \quad \text{(E-3)}$$

The component a_v given by (D-5) can then be written as

$$a_v = R\,T_r\left[\left(\frac{r_v}{r_v + r_0}\right)\ln\!\left(\frac{r_v}{r_r}\right) - \ln\!\left(\frac{r_v + r_0}{r_r + r_0}\right)\right]. \quad \text{(E-4)}$$

This formulation of a_v has already been derived in the exergetic analysis of moist-air processes described (in German) in Szargut and Styrylska (1969, Eq. (10)) and recalled in Bejan (2016, Eq. (5.48), p.207), though with different notations.

The bracketed terms in (E-4) only depend on r_v and on the two known reference values T_r and p_r, since the reference mixing ratio is $r_r = r_0\,e_r(T_r)/[\,p_r - e_r(T_r)\,]$. Therefore, a_v will be called the water-vapor component of a_m.

The impacts of q_l and q_i are not neglected up to this point, because the condensed water contents impact

Table E-1: *The ratio $|X_v/Y_v| = [p_r - e_r(T_r)]/e_r(T_r)$ computed for several reference temperatures T_r and pressures p_r. See the Table 2 for values of $e_r(T_r)$.*

$|X_v/Y_v|$	367.8 hPa	**800** hPa	1000 hPa
250 K	438	953	1193
270 K	77	169	212
273.15 K	59	130	163
280 K	36	80	100
300 K	9.4	22	27
350 K	–	0.94	1.4

the gas constant R, which depends on q_v and $q_d = 1 - q_v - q_l - q_i$. Conversely, the bracketed terms in (E-4), which generates the quadratic-like part of a_v, do not depend on q_l or q_i. These results could not be expected and are just imposed by the exact computations.

Let us introduce the water variables

$$Z_v = \frac{e}{p} = \frac{r_v}{r_v + r_0} \; , \quad Z_r = \frac{e_r}{p_r} = \frac{r_r}{r_r + r_0} \; . \qquad \text{(E-5)}$$

which are computed with (E-3). The water component a_v given by (E-4) can be transformed into the sum of the two terms depending on the function H, leading to

$$a_v = R\, T_r\, Z_r\, H(X_v) + R\, T_r\, (1 - Z_r)\, H(Y_v), \quad \text{(E-6)}$$

where

$$X_v \;=\; \frac{Z_v}{Z_r} - 1 \;=\; \frac{r_0}{r_r}\left(\frac{r_v - r_r}{r_v + r_0}\right), \qquad \text{(E-7)}$$

$$Y_v \;=\; \frac{(1 - Z_v)}{(1 - Z_r)} - 1 \;=\; -\left(\frac{r_v - r_r}{r_v + r_0}\right). \qquad \text{(E-8)}$$

The equality of (E-6) with (E-4) can be checked by using basic algebra. This result has been obtained via a lengthy trial and error process, with the aim of introducing any of the quadratic-like functions F or H of the variable $(r_v - r_r)/r_r$.

The ratio $|X_v/Y_v| = r_0/r_r = [\, p_r - e_r(T_r)\,]/e_r(T_r)$ shown in Table E-1 is computed for the set of reference values T_r and p_r used in Tables 1 and 2. The ratio is larger than 20 for $T_r \leq 300$ K and $p_r = 800$ or 1000 hPa. This result justifies the name "large" and "small" given to X_v and Y_v, respectively.

The higher temperature $T_r = 350$ K leads to small values of $|X_v/Y_v|$ which are close to unity, with an undefined (negative) ratio for 367.8 hPa. Values of $T_r > 300$ K are thus beyond the scope of the next definition for the water component of the exergy norm, where both r_v and r_r are much lower than $r_0 \approx 622$ g kg^{-1}

only for $T_r \leq 300$ K, leading to $X_v \approx (r_v - r_r)/r_r$ and $Y_v \approx -(r_v - r_r)/r_0$. The best candidate for a water dimensionless variable similar to $X_T = (T - T_r)/T_r$ is thus the large component X_v.

App. F. Separating properties of F and H.

Previous results cannot be used as such by replacing the terms $(T - T_r)^2$, $(p_s - p_r)^2$ and $(r_v - r_r)^2$ by the departure terms $(T')^2$, $(p_s')^2$ and $(r_v')^2$, respectively. This issue is motivated by the usual applications where the perturbation terms T', p_s' and r_v' may need to get zero average values, whereas $T - T_r$, $p_s - p_r$ and $r_v - r_r$ cannot cancel for all vertical levels and for constant values of T_r, p_r and r_r.

It is thus important to introduce the mean values $\overline{T}$, $\overline{p_s}$ and $\overline{r_v}$ which denote averages of T, p_s and r_v computed for a given circle of latitudes, or for a given pressure level, or for any other kind of average like those considered in Fig. F1. The eddy departure terms will then be defined in the usual way by $T' = T - \overline{T}$, $p_s' = p_s - \overline{p_s}$ and $r_v' = r_v - \overline{r_v}$.
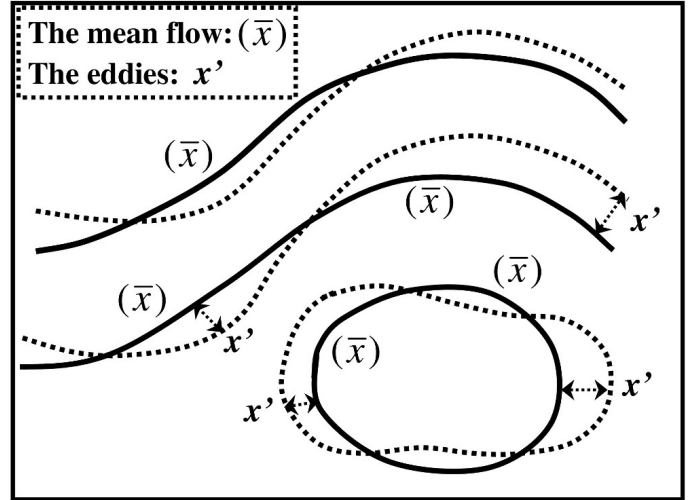

Figure F-1: *The separation of the flow into an uneven basic state ($\overline{x}$, solid lines) plus the eddies (dashed lines), defined by $x' \equiv x - \overline{x}$. The x term stands for the meteorological variables T, p, Z_v or r_v, also u and v.*

Therefore, the aim is to express the available-enthalpy functions a_T, a_p and a_v depending on $T - T_r$, $p_s - p_r$ and $r_v - r_r$ in terms of the "energies of the mean state" which depend on $(\overline{T} - T_r)^2/2$, $(\overline{p_s} - p_r)^2/2$ and $(\overline{r_v} - r_r)^2/2$ plus the "energies of the eddies" which depend on $\overline{(T')^2}/2$, $\overline{(p_s')^2}/2$ and $\overline{(r_v')^2}/2$.

For pure quadratic quantities, such as the kinetic

energy, the basic separating property is given by the binomial law

$$(X_1 + X_2)^2 = (X_1)^2 + (X_2)^2 + 2 X_1 X_2 . \quad \text{(F-1)}$$

If the flow X is separated into a mean part X_1 for which $\overline{X_1} \equiv X_1$, plus an eddy part X_2 for which $\overline{X_2} \equiv 0$, the separating property writes

$$\overline{(X_1 + X_2)^2} = \overline{(X_1)^2} + \overline{(X_2)^2} . \quad \text{(F-2)}$$

A similar exact separating property is derived for $F(X)$ in Marquet (1991, 2003), and the one valid for $H(X)$ is shown in this Appendix. For any variable written as $X = X_1 + X_2 + X_1 X_2$ the two properties

$$F(X) = F(X_1) + F(X_2) + X_1 X_2 , \quad \text{(F-3)}$$
$$H(X) = (1 + X_2) H(X_1) + (1 + X_1) H(X_2) + X_1 X_2 , \quad \text{(F-4)}$$

are valid for $X_1 > -1$ and $X_2 > -1$, which means $X_1 + X_2 + X_1 X_2 = (1 + X_1)(1 + X_2) - 1 > -1$. The flow X is then separated into the same mean and eddy parts used to derived (F-2) and with $\overline{X_1} \equiv X_1$ and $\overline{X_2} \equiv 0$, leading to

$$\overline{F(X)} = \overline{F(X_1)} + \overline{F(X_2)} , \quad \text{(F-5)}$$
$$\overline{H(X)} = \overline{H(X_1)} + (1 + \overline{X_1}) \ \overline{H(X_2)} . \quad \text{(F-6)}$$

The physical consequence of (F-2), (F-5) and (F-6) is the appearance of exact self-similarity properties verified by the total, mean and eddy parts of the flow: quadratic F or H functions generate quadratic F or H functions for the mean and the eddy parts of the flow. More precisely, the quadratic approximation of (F-5) will allow computations of $(T - T_r)^2/2$ in terms of $(\overline{T} - T_r)^2/2$ and $(T')^2/2$, with similar results derived from (F-6) and valid for surface pressure and water-vapor mixing ratio.

App. G. Mean and eddy components of a_T, a_p, a_v.

Mean and eddy components of a_T given by (C-1) can be computed by replacing $X_T = T/T_r - 1$ in (C-2) by

$$X_T = \left(\frac{T'}{\overline{T}} \right) + \left(\frac{\overline{T}}{T_r} - 1 \right) + \left(\frac{T'}{\overline{T}} \right) \left(\frac{\overline{T}}{T_r} - 1 \right), \quad \text{(G-1)}$$

where $\overline{T}/T_r - 1$ and $T/\overline{T} - 1 = T'/\overline{T}$ correspond to X_1 and X_2 in (F-5), respectively. It is then assumed that $c_p \approx c_{pd}$ and $F(X) \approx X^2/2$, leading to

$$\overline{a_T} \approx c_{pd} T_r F\left(\frac{\overline{T}}{T_r} - 1 \right) + c_{pd} T_r \overline{F\left(\frac{T'}{\overline{T}} \right)}, \quad \text{(G-2)}$$

$$\overline{a_T} \approx c_{pd} \frac{(\overline{T} - T_r)^2}{2 T_r} + c_{pd} \left(\frac{T_r}{\overline{T}} \right)^2 \frac{\overline{(T')^2}}{2 T_r} . \quad \text{(G-3)}$$

The three dimensional integral of the first quadratic term in the r.h.s. of (G-3) represents the "unavailable enthalpy" of the mean state $\overline{T}$ with respect to the isothermal reference state T_r. The integral of the second quadratic term represents the "available enthalpy" of the perturbations T' of the actual state T with respect to the mean state $\overline{T}$, and it forms the temperature contribution of the squared norm which can be written as

$$N_T \equiv \iiint \frac{c_{pd} T_r}{(\overline{T})^2} \frac{(T')^2}{2} \frac{dm}{\Sigma} . \quad \text{(G-4)}$$

This squared norm is studied in Sections 2.3 and 4.2.

The integral of a_p given by (D-7) is computed by assuming that $R \approx R_d$, leading to

$$A_p \approx R_d T_r p_r \iint \left[\int_0^{p_s} \frac{\partial H(X_p)}{\partial p} \frac{dp}{g} \right] \frac{d\Sigma}{\Sigma} , \quad \text{(G-5)}$$

$$A_p \approx R_d T_r \iint [H(X_{p_s}) - 1] \frac{p_r}{g} \frac{d\Sigma}{\Sigma} , \quad \text{(G-6)}$$

where $X_{p_s} = p_s/p_r - 1$. The term -1 is due to $X_p = -1$ for $p = 0$ and $H(-1) = 1$, leading to a constant value $R_d T_r p_r/g$ which will not enter the definition of the squared norm component for pressure. The aim is thus to compute mean and eddy components of

$$B_p = A_p + R_d T_r \frac{p_r}{g} \approx R_d T_r \frac{p_r}{g} \overline{H(X_{p_s})} , \quad \text{(G-7)}$$

by replacing X_{p_s} by

$$X_{p_s} = \left(\frac{p'_s}{\overline{p_s}} \right) + \left(\frac{\overline{p_s}}{p_r} - 1 \right) + \left(\frac{p'_s}{\overline{p_s}} \right) \left(\frac{\overline{p_s}}{p_r} - 1 \right), \quad \text{(G-8)}$$

where $\overline{p_s}/p_r - 1$ and $p_s/\overline{p_s} - 1 = p'_s/\overline{p_s}$ correspond to X_1 and X_2 in (F-6), respectively. The separating property (F-6) can then be applied to (G-7), leading to

$$B_p \approx R_d T_r \frac{p_r}{g} \left[H\left(\frac{\overline{p_s}}{p_r} - 1 \right) + \left(\frac{\overline{p_s}}{p_r} \right) \overline{H\left(\frac{p'_s}{\overline{p_s}} \right)} \right], \quad \text{(G-9)}$$

$$B_p \approx \frac{R_d T_r}{g \, p_r} \frac{(\overline{p_s} - p_r)^2}{2} + \frac{R_d T_r}{g \, \overline{p_s}} \frac{\overline{(p'_s)^2}}{2}, \quad \text{(G-10)}$$

where it is assumed that $H(X) \approx X^2/2$.

The first quadratic term of B_p in the r.h.s. of (G-10) represents the unavailable enthalpy of the mean

22

state $\overline{p_s}$ with respect to the constant reference pressure p_r. The second quadratic term represents the available enthalpy of the perturbations p'_s of the actual state p_s with respect to the mean state $\overline{p_s}$. This pressure contribution of the squared norm can be transformed back into a three dimensional integral, leading to

$$N_p \equiv \frac{R_d\,T_r}{g\,\overline{p_s}}\,\frac{\overline{(p'_s)^2}}{2} = \iint \frac{R_d\,T_r}{(\overline{p_s})^2}\,\frac{p_s}{g}\,\frac{\overline{(p'_s)^2}}{2}\,\frac{d\Sigma}{\Sigma}, \quad \text{(G-11)}$$

$$N_p = \iint \frac{R_d\,T_r}{(\overline{p_s})^2}\left(\int_0^{p_s}\frac{dp}{g}\right)\frac{\overline{(p'_s)^2}}{2}\,\frac{d\Sigma}{\Sigma}, \quad \text{(G-12)}$$

$$N_p = \iiint \frac{R_d\,T_r}{(\overline{p_s})^2}\,\frac{\overline{(p'_s)^2}}{2}\,\frac{dm}{\Sigma}\,. \quad \text{(G-13)}$$

This squared norm is studied in Section 2.3.

It is shown in Appendix E that the first term in the r.h.s. of (E-6) is much larger than the second term, due to $|X_v| \gg |Y_v|$. This result is used together with the assumptions $R \approx R_d$, $r_0 \gg r_v$ and $r_0 \gg r_r$, leading to $Z_v \approx r_v/r_0$, $Z_r \approx r_r/r_0$ and $X_v \approx r_v/r_r - 1$, to approximate the (isobaric, horizontal or uneven) surface mean value of a_v by

$$\overline{a_v} \approx R_v\,T_r\,r_r\,\overline{H\left(\frac{r_v}{r_r} - 1\right)}, \quad \text{(G-14)}$$

where $R_v = R_d/r_0$ has been used.

The separating property (F-6) can then be applied to (G-14) and with the exact property

$$\left(\frac{r_v}{r_r} - 1\right) = \left(\frac{r'_v}{\overline{r_v}}\right) + \left(\frac{\overline{r_v}}{r_r} - 1\right) + \left(\frac{r'_v}{\overline{r_v}}\right)\left(\frac{\overline{r_v}}{r_r} - 1\right), \text{(G-15)}$$

where $r'_v = r_v - \overline{r_v}$. The terms $\overline{r_v}/r_r - 1$ and $r_v/\overline{r_v} - 1 = r'_v/\overline{r_v}$ correspond to X_1 and X_2 in (F-6), respectively, with the property $\overline{r'_v} = 0$ leading to

$$\overline{a_v} \approx R_v\,T_r\,r_r\left[H\left(\frac{\overline{r_v}}{r_r} - 1\right) + \left(\frac{\overline{r_v}}{r_r}\right)\overline{H\left(\frac{r'_v}{\overline{r_v}}\right)}\right]. \text{(G-16)}$$

It is finally assumed that $H(X) \approx X^2/2$, leading to

$$\overline{a_v} \approx \frac{R_v\,T_r}{r_r}\,\frac{(\overline{r_v} - r_r)^2}{2} + \frac{R_v\,T_r}{\overline{r_v}}\,\frac{\overline{(r'_v)^2}}{2}\,. \quad \text{(G-17)}$$

The integral of the first quadratic term in the r.h.s. of (G-17) represents the unavailable enthalpy of the mean state $\overline{r_v}$ with respect to the constant reference pressure r_r. The integral of the second quadratic term represents the available enthalpy of the perturbations r'_v of the actual state r_v with respect to the mean state

$\overline{r_v}$, and it forms the water contribution of the squared norm, which can be written as

$$N_v \equiv \iiint \frac{R_v\,T_r}{\overline{r_v}}\,\frac{(r'_v)^2}{2}\,\frac{dm}{\Sigma}\,. \quad \text{(G-18)}$$

This squared norm is studied in Sections 2.3, 4.1, 4.3 and 4.5.

If the exact moist value $R = (1 - q_t)\,R_d + q_v\,R_v$ was not approximated by R_d in (E-6), leading to $R_d/r_0 = R_v$ in (G-14)-(G-17), then a factor $(1 + 2\,\delta\,\overline{r_v})$ would exist (computations not shown) in the factor of R_v in (G-18), but leading to small terms in comparison with the definition (G-18) for N_v.

References

Baker, N. L., and R. Daley, 2000: Observation and background adjoint sensitivity in the adaptive observation targeting problem. *Quart. J. Roy. Meteorol. Soc.*, **126 (565)**, 1431–1454, doi:10.1002/qj.49712656511.

Barkmeijer, J., F. Bouttier, and M. Van Gijzen, 1998: Singular vectors and estimates of the analysis-error covariance metric. *Quart. J. Roy. Meteorol. Soc.*, **124 (549)**, 1695–1713, doi:10.1002/qj.49712454916.

Barkmeijer, J., R. Buizza, T. N. Palmer, K. Puri, and J.-F. Mahfouf, 2001: Tropical singular vectors computed with linearized diabatic physic. *Quart. J. Roy. Meteorol. Soc.*, **127 (572)**, 685–708, doi: 10.1002/qj.49712757221.

Bejan, A., 2016: *Advanced engineering thermodynamics*, 740 pp. John Wiley & Sons, Inc.

Borderies, M., O. Caumont, J. Delanoë, V. Ducrocq, N. Fourrié, and P. Marquet, 2019: Impact of airborne cloud radar reflectivity data assimilation on kilometre-scale numerical weather prediction analyses and forecasts of heavy precipitation events. *Nat. Hazards Earth Syst. Sci.*, **19 (4)**, 907–926, doi: 10.5194/nhess-19-907-2019.

Buizza, R., and T. N. Palmer, 1995: The singular-vector structure of the atmospheric global circulation. *J. Atmos. Sci.*, **52 (9)**, 1434–1456, doi:10.1175/1520-0469(1995)052⟨1434:TSVSOT⟩2.0.CO;2.

Buizza, R., T. N. Palmer, J. Barkmeijer, R. Gelaro, and J.-F. Mahfouf, 1996: Singular vector, norms and

large-scale condensation. *11th Conference on numerical weather prediction*, Norfolk, Virginia, American Meteorological Society, 50-52.

Buizza, R., J. Tribbia, F. Molteni, and T. N. Palmer, 1993: Computation of optimal unstable structures for a numerical weather prediction model. *Tellus A*, **45 (5)**, 388–407, doi:10.1034/j.1600-0870.1993.t01-4-00005.x.

Cardinali, C., 2009: Monitoring the observation impact on the short-range forecast. *Q. J. R. Meteorol. Soc.*, **135 (638)**, 239–250, doi:10.1002/qj.366.

Chambon, P., L.-F. Meunier, F. Guillaume, J.-M. Piriou, R. Roca, and J.-F. Mahfouf, 2015: Investigating the impact of the water-vapour sounding observations from saphir on board megha-tropiques for the arpege global model. *Q. J. R. Meteorol. Soc.*, **141 (690)**, 1769–1779, doi:10.1002/qj.2478.

Côté, J., J.-G. Desmarais, S. Gravel, A. Méthot, A. Patoine, M. Roch, and A. Staniforth, 1998a: The operational CMC-MRB global environmental multiscale (GEM) model. Part II: Results. *Mon. Wea. Rev.*, **126 (6)**, 1397–1418, doi:10.1175/1520-0493(1998)126⟨1397:TOCMGE⟩2.0.CO;2.

Côté, J., S. Gravel, A. Méthot, A. Patoine, M. Roch, and A. Staniforth, 1998b: The operational CMC-MRB global environmental multiscale (GEM) model. Part I: Design considerations and formulation. *Mon. Wea. Rev.*, **126 (6)**, 1373–1395, doi:10.1175/1520-0493(1998)126⟨1373:TOCMGE⟩2.0.CO;2.

Courtier, P., 1987: *Application du contrôle optimal à la prévision numérique en Météorologie (Application of the optimal control to the numerical forecast in meteorology)*. PhD-thesis, Paris-VI University, France.

Courtier, P., C. Freyder, J.-F. Geleyn, F. Rabier, and M. Rochas, 1991: The arpege project at meteo france. *Seminar on Numerical Methods in Atmospheric Models, 9-13 September 1991*, ECMWF, Shinfield Park, Reading, ECMWF, Vol. II, 193-232, URL https://www.ecmwf.int/node/8798.

Courtier, P., J.-N. Thépaut, and A. Hollingsworth, 1994: A strategy for operational implementation of 4D-Var, using an incremental approach. *Quart. J. Roy. Meteorol. Soc.*, **120 (519)**, 1367–1387, doi:10.1002/qj.49712051912.

Cover, T. M., and J. A. Thomas, 1991: *Elements of Information Theory*, 563 pp. John Wiley & Sons, Inc.

Derber, J., and F. Bouttier, 1999: A reformulation of the background error covariance in the ECMWF global data assimilation system. *Tellus A*, **51 (2)**, 195–221, doi:10.1034/j.1600-0870.1999.t01-2-00003.x.

Descamps, L., D. Ricard, A. Joly, and P. Arbogast, 2007: Is a real cyclogenesis case explained by generalized linear baroclinic instability? *J. Atmos. Sci.*, **64 (12)**, 4287–4308, doi:10.1175/2007JAS2292.1.

Ehrendorfer, M., 2000: The total energy norm in a quasigeostrophic model. *J. Atmos. Sci.*, **57 (10)**, 3443–3451, doi:10.1175/1520-0469(2000)057⟨3443:NACTEN⟩2.0.CO;2.

Ehrendorfer, M., and R. M. Errico, 1995: Mesoscale predictability and the spectrum of optimal perturbations. *J. Atmos. Sci.*, **52 (20)**, 3475–3500, doi:10.1175/1520-0469(1995)052⟨3475:MPATSO⟩2.0.CO;2.

Ehrendorfer, M., R. M. Errico, and K. D. Reader, 1999: Singular-vector perturbation growth in a primitive equation model with moist physics. *J. Atmos. Sci.*, **56 (11)**, 1627–1648, doi:10.1175/1520-0469(1999)056⟨1627:SVPGIA⟩2.0.CO;2.

Ehrendorfer, M., and J. Tribbia, 1997: Optimal prediction of forecast error covariances through singular vectors. *J. Atmos. Sci.*, **54 (2)**, 286–313, doi:10.1175/1520-0469(1997)054⟨0286:OPOFEC⟩2.0.CO;2.

Ehrendorfer, M., J. J. Tribbia, and R. M. Errico, 1995: Mesoscale predictability: an assessment through adjoint methods. *Seminar on predictability*, ECMWF, 157-183, URL https://www.ecmwf.int/node/9270.

Eriksson, K.-E., and K. Lindgren, 1987: Structural information in self-organizing systems. *Physica Scripta*, **35 (3)**, 388–397, doi:10.1088/0031-8949/35/3/026.

Eriksson, K.-E., K. Lindgren, and B. Å. Månsson, 1987: *Structure, Context, Complexity, Organization: physical aspects of information and value*, 446 pp. World Scientific Publishing Co. Pte. Ltd., Singapore.

Errico, R. M., 2000: Interpretations of the total energy and rotational energy norms applied to determination of singular vectors. *Q. J. R. Meteorol. Soc.*, **126 (566)**, 1581–1599, doi:10.1002/qj.49712656602.

Errico, R. M., and M. Ehrendorfer, 1995: Moist singular vectors in a primitive-equation regional model. *10th Conference on Atmospheric and oceanic waves and stability*, Big Sky, MT, American Meteorological Society, 235-238.

Errico, R. M., K. D. Reader, and M. Ehrendorfer, 2004: Singular vectors for moisture-measuring norms. *Q. J. R. Meteorol. Soc.*, **130 (598)**, 963–987, doi:10.1256/qj.02.227.

Gauthier, P., M. Tanguay, S. Laroche, S. Pellerin, and J. Morneau, 2007: Extension of 3DVAR to 4DVAR: Implementation of 4DVAR at the Meteorological Service of Canada. *Mon. Wea. Rev.*, **135 (6)**, 2339–2354, doi:10.1175/MWR3394.1.

Gelaro, R., R. H. Langland, S. Pellerin, and R. Todling, 2010: The THORPEX observation impact intercomparison experiment. *Mon. Wea. Rev.*, **138 (11)**, 4009–4025, doi:10.1175/2010MWR3393.1.

Gelaro, R., and Coauthors, 2017: The modern-era retrospective analysis for research and applications, Version 2 (MERRA-2). *J. Clim.*, **30 (14)**, 5419–5454, doi:10.1175/JCLI-D-16-0758.1.

Holdaway, D., R. Errico, R. Gelaro, and J. G. Kim, 2014: Inclusion of linearized moist physics in NASA's Goddard earth observing system data assimilation tools. *Mon. Wea. Rev.*, **142 (1)**, 414–433, doi:10.1175/MWR-D-13-00193.1.

Holdaway, D., R. Errico, R. Gelaro, J. G. Kim, and R. Mahajan, 2015: A linearized prognostic cloud scheme in NASA's Goddard earth observing system data assimilation tools. *Mon. Wea. Rev.*, **143 (10)**, 4198–4219, doi:10.1175/MWR-D-15-0037.1.

Honerkamp, J., 1998: *Statistical Physics: an advanced approach with applications*, 410 pp. Springer-Verlag. Berlin Heildelberg New-York.

Janisková, M., and C. Cardinali, 2017: On the impact of the diabatic component in the forecast sensitivity observation impact diagnostics (also: ECMWF technical memorandum No. 786, 2016). *Data Assimilation for Atmospheric, Oceanic and Hydrologic Applications*, Park, and Xu, Eds., Vol. III., Springer International Publishing, 483–511, doi: 10.1007/978-3-319-43415-5_22, URL https://www.ecmwf.int/node/16716.

Joly, A., 1995: The stability of steady fronts and the adjoint method: Nonmodal frontal waves. *J. Atmos. Sci.*, **52**, 3082–3108, doi:10.1175/1520-0469(1995)052⟨3082:TSOSFA⟩2.0.CO;2.

Joly, A., and A. J. Thorpe, 1991: The stability of time-dependent flows: An application to fronts in developing baroclinic waves. *J. Atmos. Sci.*, **48**, 163–183, doi:10.1175/1520-0469(1991)048⟨0163:TSOTDF⟩2.0.CO;2.

Karbou, F., E. Gérard, and F. Rabier, 2010: Global 4DVAR assimilation and forecast experiments using AMSU observations over land. Part I: impacts of various land surface emissivity parameterizations. *Wea. Forecasting*, **25**, 5–19, doi:10.1175/2009WAF2222243.1.

Karlsson, S., 1990: *Energy, Entropy and Exergy in the atmosphere*. PhD-thesis, Institute of Physical Resource Theory, Chalmers University of Technology. Göteborg, Sweden, URL https://core.ac.uk/download/pdf/70599863.pdf, 121 Pp.

Kleeman, R., 2002: Measuring dynamical prediction utility using relative entropy. *J. Atmos. Sci.*, **59 (13)**, 2057–2072, doi:10.1175/1520-0469(2002)059⟨2057:MDPUUR⟩2.0.CO;2.

Kleist, D. T., D. F. Parrish, J. C. Derber, R. Treadon, W.-S. Wu, and S. Lord, 2009: Introduction of the GSI into the NCEP global data assimilation system. *Wea. Forecasting*, **24 (6)**, 1691–1705, doi:10.1175/2009WAF2222201.1.

Kullback, S., 1959: *Information theory and statistics (1978, Dover Pub.)*, 409 pp. John Wiley & Sons, Inc.

Kullback, S., and R. A. Leibler, 1951: On information and sufficiency. *Ann. Math. Statist.*, **22**, 79–86, doi:10.1214/aoms/1177729694.

Langland, R., and N. Baker, 2004: Estimation of observation impact using the NRL atmospheric variational data assimilation adjoint system. *Tellus A*, **56**, doi:10.3402/tellusa.v56i3.14413.

Lorenz, E. N., 1955: Available potential energy and the maintenance of the general circulation. *Tellus*, **7**, doi:10.3402/tellusa.v7i2.8796.

Lorenz, E. N., 1978: Available energy and the maintenance of a moist circulation. *Tellus*, **30**, doi:10.3402/tellusa.v30i1.10308.

Lorenz, E. N., 1979: Numerical evaluation of moist available energy. *Tellus*, **31**, doi:10.3402/tellusa.v31i3.10429.

Mahfouf, J.-F., and B. Bilodeau, 2007: Adjoint sensitivity of surface precipitation to initial conditions. *Mon. Wea. Rev.*, **135**, doi:10.1175/MWR3439.1.

Mahfouf, J.-F., and R. Buizza, 1996: On the inclusion of physical processes in linear forward and adjoint models. Impact of large-scale condensation on singular vectors. *Newsletter Number 72*, ECMWF, 2-6, URL https://www.ecmwf.int/node/14652.

Mahfouf, J.-F., R. Buizza, and R. M. Errico, 1996: Strategy for including physical processes in the ECMWF variational data assimilation system. *Workshop on non-linear aspects of data assimilation*, ECMWF, 595-632, URL https://www.ecmwf.int/node/10924.

Majda, A. J., R. Kleeman, and D. Cai, 2002: A mathematical framework for quantifying predictability through relative entropy. *Methods Appl. Anal.*, **9 (3)**, 425–444.

Margules, M., 1910: The mechanical equivalent of any given distribution of atmospheric pressure, and the maintenance of a given difference in pressure (Translation by C. Abbe of a lecture read at the meeting of the imperial academy of science, Vienna, July, 11, 1901). *Smithsonian Miscellaneous collections.*, **51 (4)**, 501–532, URL https://www3.nd.edu/~powers/ame.20231/gibbs1873b.pdf.

Marquet, P., 1991: On the concept of exergy and available enthalpy: Application to atmospheric energetics. *Quart. J. Roy. Meteorol. Soc.*, **117 (499)**, 449–475, doi:10.1002/qj.49711951112, URL https://arxiv.org/abs/1402.4610.

Marquet, P., 1993: Exergy in meteorology: definition and properties of moist available enthalpy. *Quart. J. Roy. Meteorol. Soc.*, **119 (511)**, 567–590, doi:10.1002/qj.49711951112, URL https://arxiv.org/abs/1807.05830.

Marquet, P., 2003: The available-enthalpy cycle. I: Introduction and basic equations. *Quart. J. Roy. Meteorol. Soc.*, **129 (593)**, 2445–2466, doi:10.1256/qj.01.62, URL https://arxiv.org/abs/1403.5671.

Marquet, P., and T. Dauhut, 2018: Reply to "comments on 'a third-law isentropic analysis of a simulated hurricane'". *J. Atmos. Sci.*, **75 (10)**, 3735–3747, doi:10.1175/JAS-D-18-0126.1, URL https://arxiv.org/abs/1805.00834.

Palmer, T. N., R. Gelaro, J. Barkmeijer, and R. Buizza, 1998: Singular-vectors, metrics, and adaptive observations. *J. Atmos. Sci.*, **55 (4)**, 633–653, doi:doi:10.1175/1520-0469(1998)055⟨0633:SVMAAO⟩2.0.CO;2.

Pearce, R. P., 1978: On the concept of available potential energy. *Q. J. R. Meteorol. Soc.*, **104 (441)**, 737–755, doi:10.1002/qj.49710444115.

Procaccia, I., and R. D. Levine, 1976: Potential work: A statistical-mechanical approach for systems in disequilibrium. *J. Chem. Phys.*, **65 (8)**, 3357–3364, doi:10.1063/1.433482.

Putman, W., 2007: *Development of the finite-volume dynamical core on the cubed-sphere*. PhD-thesis, Florida State University, U.S.A., URL https://diginole.lib.fsu.edu/islandora/object/fsu%3A168667, 91 Pp.

Rabier, F., E. Klinker, P. Courtier, and A. Hollingsworth, 1996: Sensitivity of forecast errors to initial conditions. *Q. J. R. Meteorol. Soc.*, **122 (529)**, 121–150, doi:10.1002/qj.49712252906.

Rivière, O., G. Lapeyre, and O. Talagrand, 2009: A novel technique for nonlinear sensitivity analysis: Application to moist predictability. *Q. J. R. Meteorol. Soc.*, **135 (643)**, 1520–1537, doi:10.1002/qj.460.

Shannon, C. E., 1948: A mathematical theory of communication. *Bell System Technical Journal*, **27 (3)**, 379–423, doi:10.1002/j.1538-7305.1948.tb01338.x.

Szargut, J., and T. Styrylska, 1969: Die exergetische Analyse von Prozessen der feuchten Luft (An exergetic analysis of processes for damp air). *Heiz.-Lüft.-Haustechn.*, **20 (5)**, 173–178.

Talagrand, O., 1981: A study of the dynamics of four-dimensional data assimilation. *Tellus.*, **33 (1)**, 43–60, doi:10.3402/tellusa.v33i1.10693.

Thépaut, J.-N., and P. Courtier, 1991: Four-dimensional variational data assimilation using the adjoint of a multilevel promitive-equation model. *Q. J. R. Meteorol. Soc.*, **117 (502)**, 1225–1254, doi: 10.1002/qj.49711750206.

Thomson, W., 1853: On the restoration of mechanical energy from an unequally heated space. *Phil. Mag.*, **5 (30, 4e series)**, 102–105.

Trémolet, Y., 2008: Computation of observation sensitivity and observation impact in incremental variational data assimilation. *Tellus A*, **60 (5)**, 964–978, doi:10.1111/j.1600-0870.2008.00349.x.

Wu, W.-S., R. J. Purser, and D. F. Parrish, 2002: Three-dimensional variational analysis with spatially inhomogeneous covariances. *Mon. Wea. Rev.*, **130 (12)**, 2905–2916, doi:10.1175/1520-0493(2002) 130⟨2905:TDVAWS⟩2.0.CO;2.

Xu, Q., 2006: Measuring information content from observations for data assimilation: relative entropy versus Shannon entropy difference. *Tellus A*, **59 (2)**, 198–209, doi:10.1111/j.1600-0870.2006.00222.x.

Zadra, A., M. Buenner, S. Laroche, and J.-F. Mahfouf, 2004: Impact of the GEM model simplified physics on extratropical singular vectors. *Q. J. R. Meteorol. Soc.*, **130 (602)**, 2541–2569, doi:10.1256/qj.03.208.